Additional Insights into the Design of Cr(III) Phosphorescent Emitters Using 6-Membered Chelate Ring Bis(imidazolyl) Didentate Ligands

Benchohra, Amina; Chong, Julien; Cruz, Carlos M.; Besnard, Céline; Guenee, Laure; Rosspeintner, Arnulf; Piguet, Claude

How to cite

BENCHOHRA, Amina et al. Additional Insights into the Design of Cr(III) Phosphorescent Emitters Using 6-Membered Chelate Ring Bis(imidazolyl) Didentate Ligands. In: Inorganic chemistry, 2024, vol. 63, n° 8, p. 3617–3629. doi: 10.1021/acs.inorgchem.3c03422

This publication URL: https://archive-ouverte.unige.ch/unige:175516

Publication DOI: 10.1021/acs.inorgchem.3c03422

Publication: *Inorg. Chem.* **2024**, *63*, 3617-3629. DOI 10.1021/acs.inorgchem.3c03422

Additional insights into the design of Cr(III) phosphorescent emitters using 6-membered chelate ring bis(imidazolyl) didentate ligands[**]

*Amina Benchohra**[a], Julien Chong[a], Carlos Moreno Cruz[b,c], Céline Besnard[d], Laure Guénée[d], Arnulf Rosspeintner[e] and Claude Piguet**[a]*

---

[a] Dr Amina Benchohra, Mr Julien Chong, Prof. Dr Claude Piguet
Department of Inorganic, Analytical and Applied Chemistry
University of Geneva, 30 quai E. Ansermet
CH-1211 Geneva 4 (Switzerland)
Email: amina.benchohra@unige.ch, claude.piguet@unige.ch

[b] Dr Carlos Moreno Cruz
Department of Organic Chemistry, Unidad de Excelencia de Química (UEQ)
University of Granada, Avda. Fuente Nueva
ES-18071 Granada (Spain)

[c] Department of Chemistry
University of Zurich, Winterthurerstrasse 190
CH-8057 Zurich (Switzerland)

[d] Dr Céline Besnard, Dr Laure Guénée
Laboratory of Crystallography.
University of Geneva, 24 quai E. Ansermet
CH-1211 Geneva 4 (Switzerland)

[e] Dr Arnulf Rosspeintner
Department of Physical Chemistry
University of Geneva, 30 quai E. Ansermet
CH-1211 Geneva 4 (Switzerland)

[**] This work was supported through grants of the Swiss National Science Foundation.

§ Supporting information and the ORCID identification number(s) for the author(s) of this article can be found under https:/doi.org/

Keywords: homoleptic chromium(III) complexes • spin-flip phosphorescence • six-membered chelate ring • luminescent molecular materials• multifunctional chromium(III) complexes.

ABSTRACT

The interest in Cr(III) complexes has been rejuvenated over the past decades for building practical guidelines in the design of efficient earth-abundant phosphorescent near-infrared emitters. In that context, we report the first family of homoleptic tri(didentate) Cr(III) complexes $[Cr\mathbf{L}_3]^{3+}$ based on polyaromatic ligands inducing 6-membered chelate rings, namely: the bis(1-methylimidazol-2-yl)ketone (**L** = bik), bis(1-methylimidazol-2-yl)methane (**L** = bim) and bis(1-methylimidazol-2-yl)ethane (**L** = bie) ligands. The programmed close-to-perfect octahedral micro-symmetry of $\{Cr^{III}N_6\}$ chromophores found in $[Cr(bik)_3](OTf)_3$ (**1**), $[Cr(bim)_3](OTf)_3$ (**2**) and $[Cr(bie)_3](BF_4)_3$ (**3**) ensures a ligand-field strength large enough to induce intense and long-lived Cr-based phosphorescence. Impressive excited-state lifetimes (5.0-8.2 ms) were obtained at low temperature for the $[Cr(\mathbf{L})_3]^{3+}$ series. Additionally, the photoluminescent quantum yield climbs to 0.8% for (**1**) in deaerated solutions. Moreover, the photophysical features of the three homoleptic complexes are barely influenced by the presence of dioxygen presumably because of the poor overlap between the Cr-based phosphorescence spectra (*c.a.* 14100 cm^{-1}) and the $^1\Sigma_g^+ \leftarrow {}^3\Sigma_g^-$ transition in the absorption spectrum of dioxygen (13100 cm^{-1}). The multiredox electrochemical pattern of (**1**) is evidenced by cyclic-voltammetry as well as its strong photo-oxidant behavior. The pH-sensitivity of (**2**) and (**3**) luminescence is discussed along with the reactivity of their β-diketiminate derivatives.

INTRODUCTION

The importance of the nature, size and degrees of freedom (i.e. rigidity) of the chelate metallorings for tuning the structural, thermodynamic and electronic properties of coordination complexes has been early recognized,[1] and systematically exploited for performing selective complexation processes in analytical,[2] or metallosupramolecular chemistry.[3] Since easily accessible 5-membered chelate rings, derived from flexible 1,2 diaminoethane scaffolds, appeared to be efficient for the sequestration of almost all metallic cations,[4] albeit with a slight preference for the largest ones,[3] much less attention has been focused on the synthetically more demanding 6-membered chelate rings. Further gain in structural control and preorganization relied on the introduction of rigid and planar aromatic heterocycles within the 5-membered chelate rings to give the well-known pseudo-octahedral $[M(bipy)_3]^{2+}$ (bipy = 2,2'-bipyridine) and $[M(phen)_3]^{2+}$ (phen = 1,10 phenanthroline) chromophores (Scheme 1).[3] This paved the way for the discovery of long-lived excited metal-to-ligand charge transfer state with unprecedented photochemical properties with the rarest metals M = Ru or Os.[5] Beyond the 25-fold increase in stability observed for the same entering metal upon replacing the bipy ligand with its preorganized phen counterpart,[3,4] there is no doubt that these rigid didentate receptors prefer larger cations for the formation of 5-membered chelate rings as illustrated by the larger stabilities reported for $[Ag\mathbf{L}]^+$ compared to $[Cu\mathbf{L}]^+$ in acetonitrile.[6] Interestingly, the simple $4n+2$ *Hückel* electron-counting rule assigns 2 x 6 π-electrons for bipy and 14 π-electrons (delocalized aromatic scaffold) for phen (Scheme 1), a fact that is rarely considered for the simple rationalization of the electronic properties of these ligands, probably because *Clar*'s π-sextet rule,[7] which restricts efficient aromaticity to the formation of local 6 π-electrons benzene-like rings, is now out of debate (Scheme 1).[8] According to the latter π-sextet rule, going from bipy to phen would not significantly change the fraction of local aromaticity, as it is expected to be much

larger on the outer rings than on the central one in phenanthroline. The lack of pronounced shift towards low energy for the $\pi^*\leftarrow$N(2p) and $\pi^*\leftarrow\pi$ transitions recorded in bipy and phen supports the latter analysis (Figure S1), but much less is known for the related pair of extended ligands bis(pyridin-2-yl)methane (bpm) / bis(pyridin-2-yl)ketone (bpk), which are coded for the formation of rigid 6-membered chelate metallorings[9] (Scheme 1). Interestingly, the closely related bim/bik pair[10] provides 6-membered pseudo octahedral $[Fe(bim)_3]^{2+}$ and $[Fe(bik)_3]^{2+}$ complexes with completely different electronic properties since the first one adopts a strict high-spin conformation at all temperatures, whereas $[Fe(bik)_3]^{2+}$ is spin-crossover around room-temperature.[11]

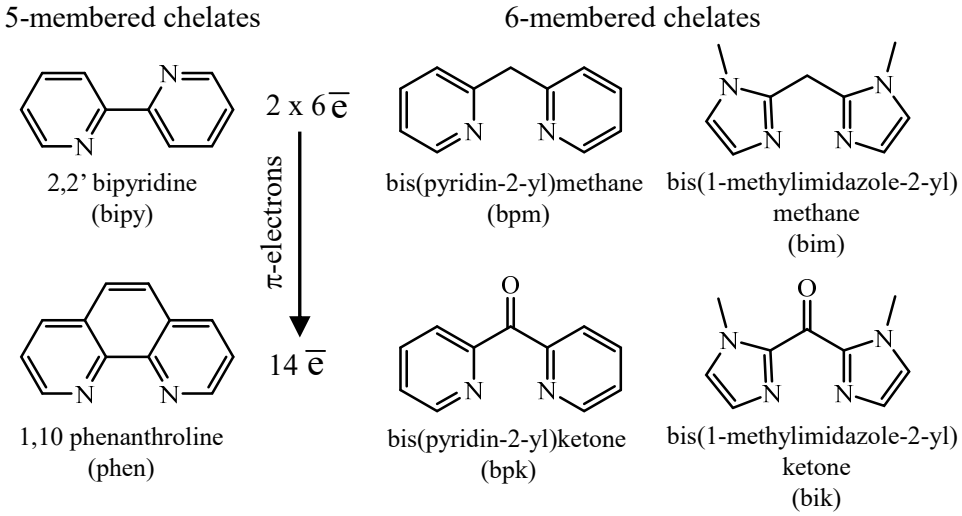

Scheme 1. Chemical structures of didentate polyaromatic ligands for the formation of 5-membered (left) or 6-membered (right) chelate metallorings.

On the other side, the quest for earth-abundant phosphorescent emitters has renewed interest for Cr(III) coordination chemistry over the past decade. Ensuing progress has in turn legitimized the potential and competitiveness of Cr(III) coordination entities for substituting precious metals in multiple (applied) research fields.[12] Recent literature has particularly laid stress on the outstanding photophysical and photochemical properties of some strong-field $\{Cr^{III}N_6\}$ molecular chromophores using di(tridentate) scaffolds forming four 6-membered chelating rings, which have

earned the label of 'molecular Ruby' and defied at times their emblematic Ru(II) analogues.[12,13] The features singularity of these pseudo-octahedral d^3-Cr(III) emitters includes a near-infrared (NIR) phosphorescence stemming from metal-centered spin-flip transitions, long-lived excited states (from μs to ms), and efficient sensitization pathways via either ligand-centered, ligand-to-metal charge transfer (LMCT) or metal-centered excitations. In its early years, research of Cr(III) emitters essentially drew on tri(didendate), and to a lesser extent di(tridentate), Cr(III) polypyridyl complexes with 5-membered chelate rings. The first generation of compounds naturally found its roots in classical polypyridyl bipy, phen and 2,2';6',2''-terpyridine (tpy) derivatives.[14] Aside from $[Cr(phen)_3]^{3+}$, these Cr(III) complex families delivered relatively low photophysical performance given their low phosphorescence lifetimes (τ) and quantum yields (*e.g.* $\phi = 0.089$ % for $[Cr(bpy)_3]^{3+}$ and < 0.001 % for $[Cr(tpy)_2]^{3+}$ in aerated water).[15] To address this issue, the NIR-luminescent Cr(III) complexes' design lately turned towards an expansion of the chelate ring, for optimizing the metal-ligand orbitals overlap concomitant to an increase of the ligand field strength.[16] One of the underlying purposes was to maximize the energy gap between the $^4T_{2g}$ and ^2E_g excited levels in order to preclude non-radiative relaxation by back-intersystem crossing (BISC) processes. A first demonstration was provided by Heinze *and coworkers*[13a),17] using an extended tridentate terpy-like ligand, the ddpd (ddpd = *N*,*N*'-dimethyl-*N*,*N*'-dipyridine-2-ylpyridine-2,6-diamine). The lifetime and quantum yield of the corresponding di(tridendate) Cr(III) complex, $[Cr(ddpd)_2]^{3+}$, remarkably reach 1.12 ms, and 13.7% in deaerated acetonitrile. Likewise, other strategic chemical designs were implemented for tuning the spin-flip emission features and relied mainly on the modulation of the interelectronic repulsion (i.e. the nephelauxetic effect), and inherently the energy of the spin-flip states. The spectral range observed for Cr(III) spin-flip emission (all categories of compounds combined) spans visible to NIR-II (670 to 1700 nm). Rigidification of the structure or

insertion of an inversion center were successfully applied for gaining control over emission lifetimes, by limiting intramolecular motions (and thus non radiative deactivation pathways) or by exploiting Laporte's rule (for influencing radiative rate constant) respectively.[18] Curiously, the $\{Cr^{III}N_6\}$ spin-flip emitters engineering has been structured in the absence of homoleptic tri(didentate) Cr(III) examples with 6-membered chelating rings. In the infancy of inorganic optical isomerism, an elusive interest was given to 1,3-propylenediamine six membered chelate ring-based systems for resolving their conformational and chiro-optical properties.[19] To the best of our knowledge, there was no further extension to the class of homoleptic tris(chelates) Cr(III) derivatives with 6-membered chelate ring. A likely reason for this lack of interest lies in their difficult preparation and characterization, given the general hurdles faced in Cr(III) chemistry. Similar considerations hold for Cr(III) heteroleptic chemistry as pointed out by sporadically emerging reports.[20] Regarding polypyridyl didentate ligands, Doistau *et al*[21] prospected the influence of the 6-membered chelating dpma (dpma = di(pyridyl-2-yl)(methyl)amine) on the ligand-field, nephelauxetic effect as well as on the spin-flip luminescence of the heteroleptic $[Cr(phen)_2(dpma)]^{3+}$ complex. To go along with these studies, we opened up the investigations on a series of homoleptic tri(didentate) Cr(III) complexes based on the set of 6-membered chelate ring bis(imidazol-2-yl) derivatives bik, bim or bie (Scheme 1 and 2). An initial glimpse of imidazole-based didentate use with Cr(III) was provided in early 2000s by Rüther *et al*.[22] Driven by the development of new homogenous catalysts for olefin polymerization, the authors notably investigated the synthesis and reactivity of $[\{Cr(N^{\cap}N)Cl_2\text{-}\mu Cl\}_2]$ (with $N^{\cap}N$ = bik or bim) dinuclear Cr(III) complexes. It is also worth acknowledging the difficulties emphasized by the authors at various points for characterizing and isolating their different Cr(III) species. The 'unique' single-crystal XRD structure obtained for the mononuclear $[Cr(bik)(CH_3CN)Cl_3]$ complex, resulted from the cleavage of $[\{Cr(bik)Cl_2\text{-}\mu Cl\}_2]$ dimers in acetonitrile. In order to

explore the potential of $\{Cr^{III}N_6\}$ spin-flip emitters possessing three 6-membered polyaromatic metallorings with variable numbers of π-electrons and associated rigidity, we detail here the in-depth investigations of the photophysical, electrochemical and acid-base properties of the $[Cr(bik)_3](OTf)_3$ (**1**), $[Cr(bim)_3](OTf)_3$ (**2**) and $[Cr(bie)_3](BF_4)_3$ (**3**) homoleptic complexes.

RESULTS AND DISCUSSION

Synthesis of the homoleptic *D*$_3$-symmetrical $[Cr(bik)_3](OTf)_3$, $[Cr(bim)_3](OTf)_3$ and *C*$_1$-symmetrical $[Cr(bie)_3](BF_4)_3$ complexes.

The bik, bim and bie derivatives were synthesized according to existing procedures with minor modifications (Scheme S1, Figures S2-S7).[23] The corresponding homoleptic Cr(III)-complexes were prepared in two steps from the chromous salt $Cr^{II}(OTf)_2{\cdot}2H_2O$.[24] The complexation reactions were carried out by mixing 3 eq of ligands with 1 eq of the chromous salt in acetonitrile at room temperature under an argon atmosphere. If the subsequent oxidation process of the $[Cr^{II}(\mathbf{L})_3](OTf)_2$ (**L**= bik, bim or bie) intermediates could be conducted in air in the case of $[Cr^{II}(bik)_3](OTf)_2$ complex, the chemical oxidation of $[Cr^{II}(bim)_3](OTf)_2$ and $[Cr^{II}(bie)_3](OTf)_2$ was performed using one-electron oxidant $NOBF_4$ (1 eq) under an inert atmosphere, or in acidic media, to avoid the compounds' over-oxidation (Figures S8 to S15). Due to the reducing character of the bis(imidazol-2-yl)methane (bim) and bis(imidazol-2-yl)ethane (bie) ligands, an 'uncontrolled' air-based oxidation resulted in their conversion into their ketone or carbinol equivalents, respectively. For instance, an intricate mixture of the homoleptic $[Cr(bim)_3]^{3+}$ and heteroleptic $[Cr(bik)_n(bim)_{3-n}]^{3+}$ (with $1 \leq n \leq 3$) complexes could be observed by low-resolution mass spectroscopy (LRMS) and infrared (IR) spectroscopy when $[Cr(bim)_3]^{2+}$ was oxidized in air. The $[Cr^{III}(bim)_3]^{3+}$ mass peak at m/z = 878.2, is indeed bordered at higher m/z ratio by the oxidized species ones, with a consistent addition of 14 units each time corresponding to the replacement of two hydrogen atoms with one

oxygen atom, *i.e.* *m*/*z* = 892.1, 906.1 and 920.0 (Figure S17). IR spectroscopy also provides evidence for ligand oxidation as the mixture spectrum presents characteristic ν_{CO} stretching vibrations at 1679 cm^{-1}, close to those observed for $[Cr^{III}(bik)_3]^{3+}$ (1657 cm^{-1}) in Figure S16. Finally, the three targeted homoleptic complexes could be isolated in moderate yields (20 to 46%), together with the concomitant formation of small amounts of dimeric hydroxo-bridged species. A recurring difficulty, general to amine/diimine chromium(III) complexes preparation, is associated to aquation phenomena and the subsequent generation of hydroxo-complexes formed in acetonitrile containing residual water from the starting $Cr^{II}(OTf)_2{\cdot}2H_2O$ salt. These latter have a marked tendency to polymerize in basic or neutral media, and even at acidic pH.[25] A result of this aquation process is represented by the $[\{Cr(bim)_2\text{-}\mu OH\}_2]^{4+}$ dimer crystal structure shown in Figure S22. The three homoleptic tri(didentate) complexes, $[Cr^{III}(bik)_3](OTf)_3$, $[Cr^{III}(bim)_3](OTf)_3$ and $[Cr^{III}(bie)_3](BF_4)_3$, were first characterized by elemental analyses, (nano-spray) HRMS, IR spectroscopy and XRD. Characteristic mass spectrometry peaks of the complexes, following the loss of an anion, were identified at *m*/*z* = 920.1011, 878.1628 and 796.3125 for $\{[Cr^{III}(bik)_3](OTf)_2\}^+$, $\{[Cr^{III}(bim)_3](OTf)_2\}^+$, $\{[Cr^{III}(bie)_3](BF_4)_2\}^+$ respectively. Suitable crystals for single-crystal XRD measurements of the three complexes were successfully achieved by diffusion of methyl tert-butyl ether in their acetonitrile solution (Scheme 2). For $[Cr(bie)_3]^{3+}$, it is interesting to note that the different wrapping combinations of bie ligands around the metal centre could in theory lead to two geometrical isomers: a C_3-symmetrical one for which methyl groups (Me_β) rotational sense is the same (*i.e.* clockwise = C or anticlockwise = A), and/or a C_1-symmetrical isomer displaying two ligands with Me_β facing each other. The equilibria of the $[Cr(bie)_3](BF_4)_3$ isomers formation are represented in Figure S18.

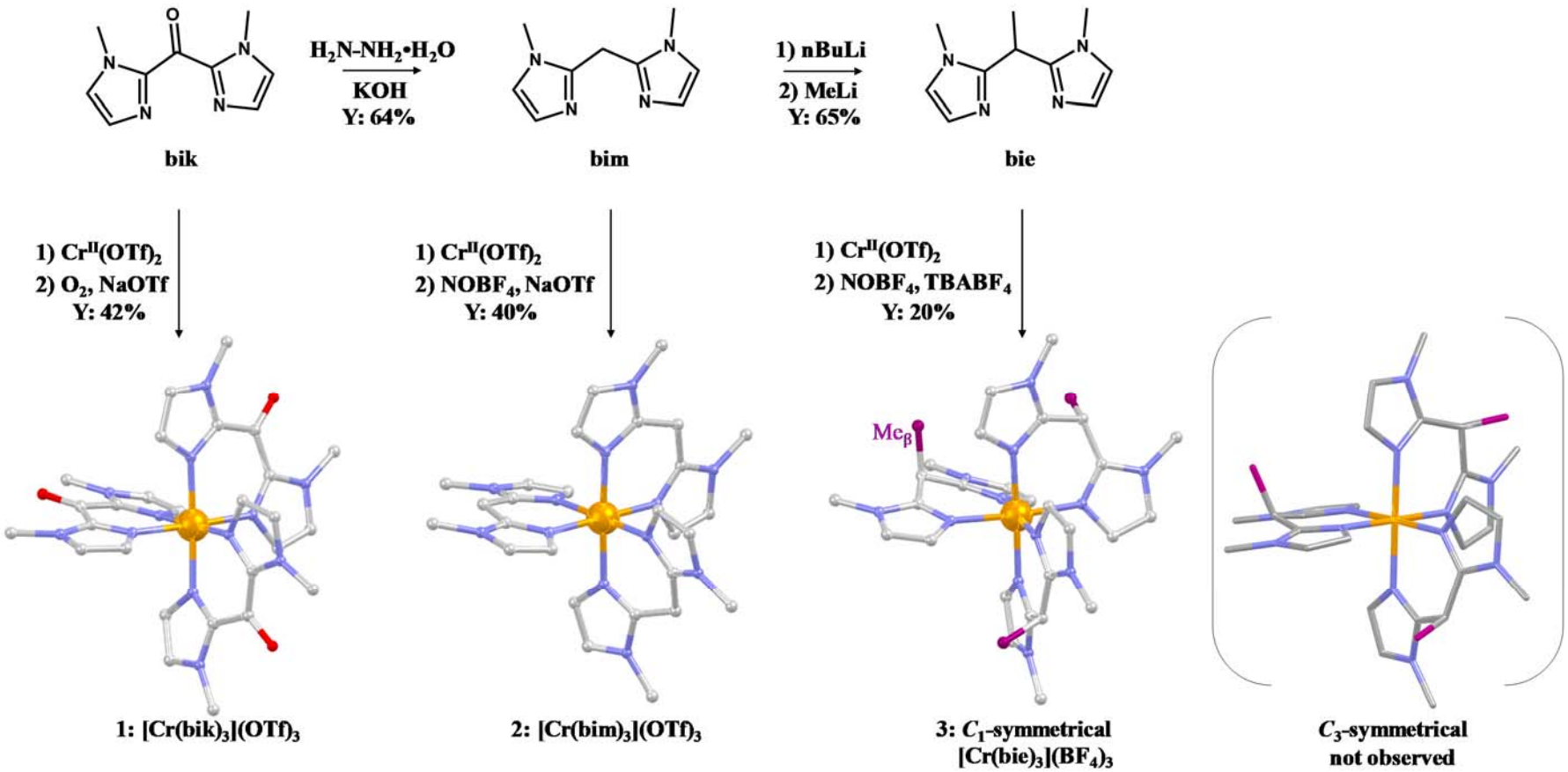

Scheme 2. Syntheses of the homoleptic $[Cr(bik)_3]^{3+}$, $[Cr(bim)_3]^{3+}$ and C_1-symmetrical $[Cr(bie)_3]^{3+}$ complexes depicted as found in their crystal structures. DFT computed optimized geometry of the C_3-symmetrical $[Cr(bie)_3]^{3+}$ isomer is represented alongside the C_1-symmetrical isomer. Carbon atoms are shown in grey (except the Me_β in C_1-symmetrical $[Cr(bie)_3]^{3+}$ highlighted in violet), N in blue, O in red and Cr in orange. Solvent, anions and hydrogen atoms are omitted for clarity.

If, in a first instance, the sequential additions of bie ligands around the metal ion are considered independent events, the probability of occurrence of C_1-symmetrical and C_3-symmetrical $[Cr(bie)_3]^{3+}$ complexes would be 0.75 and 0.25, respectively.[26] A similar outcome is deduced from the more formalistic symmetry numbers method (Figure S18), introduced by Benson in 1958 [27] and extended to supramolecular assemblies by Ercolani, Piguet and coworkers.[28] An initial single-crystal XRD measurement revealed a monoclinic structure only consisting of the C_1-symmetrical isomer. Additional analyses of four other crystals aligned with the sole presence of the lower symmetrical $[Cr(bie)_3]^{3+}$. X-ray powder diffraction (XRPD) experiment was then carried out to ensure the isolated compound was representative of the bulk sample and thus eliminate any statistical bias (*e.g.* in the crystal selection). A crystalline powder was thus prepared by 'fast-precipitation' of $[Cr(bie)_3]^{3+}$ acetonitrile solution, to approach the solution-phase composition and thus define whether the solid-phase constitution derived from a selective isomer formation or a preferential crystallization from an isomeric mixture. The powder diffractogram recorded at room temperature on the crystalline powder is depicted in Figure S26. This latter could be successfully indexed in a monoclinic (P21/n) with refined cell parameters (Lebail fit) a = 12.3708(5) Å, b = 11.8006(4) Å c = 28.6657(10) Å. The peaks, as well as their respective intensities, coincide well with the ones simulated from the C_1-symmetrical $[Cr(bie)_3]^{3+}$ crystal structure. Also, a structural resolution of the powder data (Figure S29) was performed with the program 'free objects for crystallography' (FOX) and is in line with the one determined by single-crystal structure analysis. Thus, XRPD studies corroborate an overall bulk phase exclusively comprised of the C_1-symmetrical isomer, reasonably assumed to result from a selective equilibrium distribution in solution. To account for any deviation from a statistical C_1 and C_3 isomer formation (*i.e.* cooperativity), the thermodynamic equilibria were modelled with the site-binding model.[26c] The respective stability constants, β^{C_1} and β^{C_3}, translate mathematically as eqns (1) and (2).

$$\beta^{c_1} = \omega^{c_1} \cdot \left(f_{\text{inter}}^{\text{Cr,bie}}\right)^3 \cdot \left(u^{\text{bie,bie}}\right) \cdot \left(u^{\text{bie,bie}^*}\right) \cdot \left(u^{\text{bie}^*,\text{bie}}\right) \quad (1)$$

$$\beta^{c_3} = \omega^{c_3} \cdot \left(f_{\text{inter}}^{\text{Cr,bie}}\right)^3 \cdot \left(u^{\text{bie,bie}}\right)^3 \quad (2)$$

These thermodynamic equilibrium constants are expressed as the product of three or five parameters, as the case may be: *(i)* the rotational statistical factor (ω^{c_1} or ω^{c_3}) transcribing the contributions of symmetry differences between reactants and products, and entropy of mixing to standard entropy change; *(ii)* the hetero-component connection descriptor, $f_{\text{inter}}^{\text{Cr,bie}}$, reflects the affinity of a metal for a given binding site; and *(iii)* $u^{\text{bie,bie}}$ pertains to ligand-ligand intramolecular interactions when Meβ are arranged in the same sense, while $u^{\text{bie}^*,\text{bie}}$ and $u^{\text{bie,bie}^*}$ refer to ligand-ligand intramolecular interactions when Meβ are arranged in opposite senses. Interestingly, the combination of isomers formation equilibria corresponds to the isomerization reaction, the equilibrium constant of which finds its expression, after simplification, in eqn (4). The statistical factor can be written as $\omega^{\text{Iso}} = \omega^{c_1}/\omega^{c_3}$ and calculated with the symmetry number method (Figure S18), giving $\omega^{\text{Iso}} = 3$. Therefore, there is a pure entropic contribution to the isomerization free energy of $-RT\ln(\omega^{\text{Iso}}) = -2.7$ kJ·mol^{-1} (at 300K) in favor of the *C*$_1$-symmetrical isomer, just due to the symmetry lowering.

$$C_3\text{-}[\text{Cr(bie)}_3]^{3+} \rightleftharpoons C_1\text{-}[\text{Cr(bie)}_3]^{3+} \qquad \beta^{\text{Iso}} \quad (3)$$

$$\beta^{\text{Iso}} = \frac{\beta^{c_1}}{\beta^{c_3}} = \frac{\omega^{c_1}}{\omega^{c_3}} \cdot \frac{\left(u^{\text{bie,bie}}\right)\left(u^{\text{bie,bie}^*}\right)\left(u^{\text{bie}^*,bie}\right)}{\left(u^{\text{bie,bie}}\right)^3} = \frac{48}{16} \cdot \frac{\left(u^{\text{bie,bie}^*}\right)\left(u^{\text{bie}^*,bie}\right)}{\left(u^{\text{bie,bie}}\right)^2} \quad (4)$$

Setting a maximum formation of 1% mole fraction of the *C*$_3$-symmetrical isomer in the final $[\text{Cr(bie)}_3]^{3+}$ mixture, results in $\beta^{\text{Iso}} \geq 99$ (eqn 3) and an extra stabilization of the *C*$_1$-isomer by $\Delta G_{\text{global}} = RT\ln(\beta^{\text{Iso}}/3) \geq 8.7$ kJ·mol^{-1}. A further insight was brought by theoretical

calculations on the relative energy of the C_3-and C_1-symmetrical $[Cr(bie)_3]^{3+}$ isomers, performed by DFT optimizations using the unrestricted version of the Becke three-parameters exchange function in combination with the Lee-Yang-Parr correlation functional (UB3LYP). They suggest a stabilization by 12.5 kJ·mol^{-1} of the C_1 isomer. This energy difference corresponds to $\beta^{Iso} = 466$ and the formation of only 0.2% of the C_3-symmetrical isomer at equilibrium. The origin of this energy drift can be tentatively attributed to specific intramolecular interligands interactions.[29] In the C_1 isomer, two bie ligands offer a favorable disposition to the methyl groups (Me_β) for close H···Imidazole interactions (Figure S23). In the X-ray structure, two intramolecular contacts were identified between the hydrogens (of Me_β groups) positioned orthogonally to the imidazole rings centroids, at distances of ~2.8 Å. In contrast, the simulated structure of the C_3 isomer (Figure S24) shows that all the hydrogens of Me_β are off-centered from neighbouring imidazole rings and thus do not present a directionality conducive to potential efficient H···Imidazole interactions.

Structural analyses of the homoleptic Cr(III)-complexes derived from the octahedral geometry.

The main features of the three complexes crystal structures are summarized in Table 1. Both $[Cr(bik)_3](OTf)_3$ and C_1-$[Cr(bie)_3](BF_4)_3$ crystallize as racemic mixture (of Δ/Λ enantiomers) in the monoclinic space group $P2_1/n$ with one molecule per asymmetric unit. For its part, the $[Cr(bim)_3](OTf)_3$ racemate crystal structure belongs to the monoclinic space group Pc and its asymmetric unit contains three crystallographically independent molecules (Cr_A, Cr_B and Cr_C, Figure S21). Comparative analysis of $[Cr(bik)_3](OTf)_3$, $[Cr(bim)_3](OTf)_3$ and C_1-$[Cr(bie)_3](BF_4)_3$ metal-ligand distances ($d_{Cr\text{-}N}$) and bite angles (N-Cr-N) revealed a similar $\{Cr^{III}N_6\}$ micro-symmetry for the three complexes. All complexes exhibit mean Cr-N bond lengths between 2.047(1) Å and 2.048(1) Å and mean chelate N-Cr-N bite angles (87.7°-88.1°, Figure 1a) close to

the ideal 90° for a perfect octahedron. The conformation of the 6-membered chelate rings appear slightly twisted, irrespective of the ligand, to arrange in a skew-boat manner. This point is notably reflected in the average values of ∠CrN-C_{im}N and ∠CrN-$C_{im}C_{\alpha}$ torsion angles (Figure 1c-d). The corresponding values are relatively close for $[Cr(bim)_3](OTf)_3$ (174.5° and 5.9°) and *C*1-$[Cr(bie)_3](BF_4)_3$ (173.9° and 7.7°) but show nonetheless a more pronounced chelate twist in $[Cr(bik)_3](OTf)_3$ (171.3° and 10.6°). This variation in the complexes series obviously stems from the strain imposed by the central bridging carbon (C_{α}, Figure 1b). The conformation of bim and bie ligands get significantly distorted upon complexation.

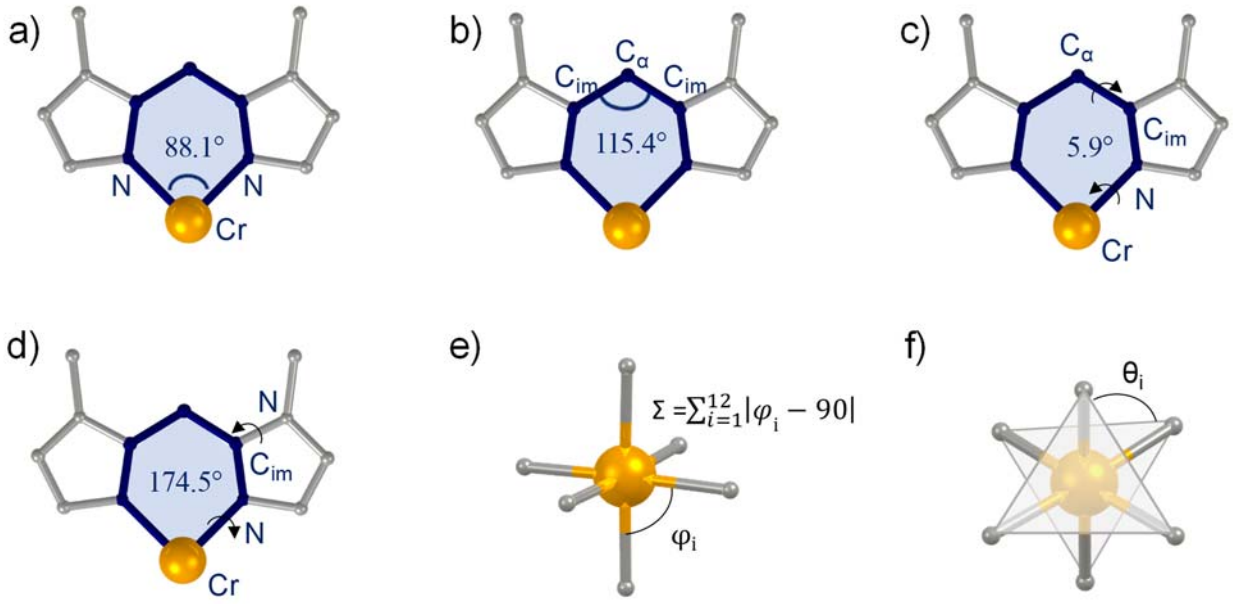

Figure 1. Definitions of selected structural parameters given in Table 1, illustrated with {Cr(bim)} fragments: bite angle (a), tetrahedral angle (b) and torsions angles (c and d). (e) and (f) represent Σ and θ parameters respectively.

The imidazole rings arrangement of a bim or bie unit approach coplanarity, *i.e*. the angles between the planes formed by the imidazole rings (interplanar angles) considerably decrease upon complexation (interplanar angles being 13.8° in $[Cr(bim)_3](OTf)_3$, 18.7° in *C*1-$[Cr(bie)_3](BF_4)_3$)

versus *ca*. 75° in free ligands) . Moreover, the C_{im}-C_{α}-C_{im} angle in those complexes amounts to 115.4° and 113.9° respectively, which is significantly higher than the normal tetrahedral angle of 109.5°. The chelate rings tend thus to flatten to alleviate the surplus of strain. However, with its sp^2 bridging carbon, bik ligand exhibits a planar structure of restricted flexibility, limiting the range of possible geometries of the chelate ring. Therefore, to accommodate the metal ion and minimize the ring-strain (with the defined Cr-N bond lengths), the system distorts along the (∠CrN-$C_{im}C_{\alpha}$ and ∠CrN-C_{im}N) torsional coordinates (Table 1).

Table 1. Structural parameters for the pseudo-octahedral CrN_6 chromophores as found in the crystal structures of the three homoleptic $[Cr(\mathbf{L})_3]^{3+}$ complexes (**L** = bik, bim or bie).

	$[Cr(bik)_3]^{3+}$	$[Cr(bim)_3]^{3+}$ [a]	$[Cr(bie)_3]^{3+}$
$d_{Cr\text{-}N}$ /Å	2.0470(13)	2.0480(7)	2.0478(3)
∠ (N-Cr-N) /°	87.7(5)	88.1(3)	88.4(10)
∠ (C_{imi}-C_{α}-C_{imi}) /°	118.2(2)	115.4(7)	113.9(3)
∠CrN-C_{im}N /°	171.3(2)	174.5(5)	173.9(2)
∠CrN-$C_{im}C_{\alpha}$ /°	10.6(1)	5.9(1)	7.7(4)
Σ [b] /°	26.03	13.3	26.52
θ [c] /°	59.8	58.0	57.8

[a] Average data of the three crystallographically independent $[Cr(bim)_3]^{3+}$ molecules in the asymmetric unit (Cr_A, Cr_B and Cr_C). [b] Σ is the sum of the deviations from 90° of the 12 *cis*(N-Cr-N) angles in the coordination sphere (Figure 1e). [c] θ is the average of the 3 twist angles along the pseudo-C_3 axis (Figure 1f).

The deformations of the $Cr^{III}N_6$ octahedron geometry were probed with the two parameters, Σ and θ, which express the coordination sphere and trigonal-twist distortions degree respectively (Figure 1e-f).[30] Thus, Σ is defined as the sum of the deviations from 90° of the twelve *cis* N-Cr-N angles

while θ is the average of trigonal twist angles (with θ = 60° for an octahedral geometry). In $[Cr(bik)_3](OTf)_3$ and C_1-$[Cr(bie)_3](BF_4)_3$ complexes, the distortion of the CrN_6 coordination environment is equivalent, with Σ values of 26.0° and 26.5° respectively. In contrast, the deformation is twice smaller in $[Cr(bim)_3](OTf)_3$ complex (Σ = 13.3°). Overall, there is no major apparent difference in $\{Cr^{III}N_6\}$ micro-symmetry of the three complexes but rather local constraints, more pronounced in $[Cr(bim)_3](OTf)_3$ and C_1-$[Cr(bie)_3](BF_4)_3$ cases (as exemplified by the pair superimpositions of the complexes depicted in Figure S25).

Photophysical properties of $[Cr(bik)_3](OTf)_3$, $[Cr(bim)_3](OTf)_3$ and $[Cr(bie)_3](BF_4)_3$.

An important aspect of Cr(III) complexes spectroscopy are the so-called 'Ruby' lines, which correspond to narrow spin-forbidden transitions observed in most trivalent chromium complexes.[31] With their [Ar]$3d^3$ electronic configuration, the Cr(III) chromophores energy diagram are in most cases sufficiently handled by the d^3 Tanabe-Sugano diagram derived for an octahedral geometry (Figure 3d). Two kinds of metal-centered transitions are conceivable: *(i)* intraconfigurational transitions defined by a change of one spin orientation within the $(t_{2g})^3$ configuration; and *(ii)* interconfigurational transitions between t_{2g} and e_g orbitals with conservation of the three spin orientations, as depicted in Figure 3d. In that respect, the lowest-energy broad spin-allowed transition, $Cr(^4T_2 \leftarrow {}^4A_2)$, was readily identified at 476 nm (ε = 65 $M^{-1}\cdot cm^{-1}$). and 482 nm (ε = 70 $M^{-1}\cdot cm^{-1}$) for $[Cr(bim)_3](OTf)_3$ (**2**) and $[Cr(bie)_3](BF_4)_3$ (**3**) complexes respectively (Figure 2), in good agreement with calculations. Since Cr(III) is neither a good oxidizing nor reducing entity, the d-d absorptions are not obscured by metal-involving charge transfer bands that are rather located in the UV part. As less distinguishable, the $Cr(^4T_2 \leftarrow {}^4A_2)$ transition assignment in $[Cr(bik)_3](OTf)_3$ (**1**) was assisted by calculations, with a maximum defined at 433 nm (ε = 332 $M^{-1}\cdot cm^{-1}$). Higher energy transitions were ascribed to internal ligand transitions or mixed ligand-centered/LMCT

transitions according to TD-DFT calculations (Figures S49 to S63). One notices a global red-shift of mixed ligand-centered/LMCT transitions in going from $[Cr(bim)_3]^{3+}$ and $[Cr(bie)_3]^{3+}$ (2 x 6 π-electrons) to $[Cr(bik)_3]^{3+}$ (14 π-electrons) (Figure 2).

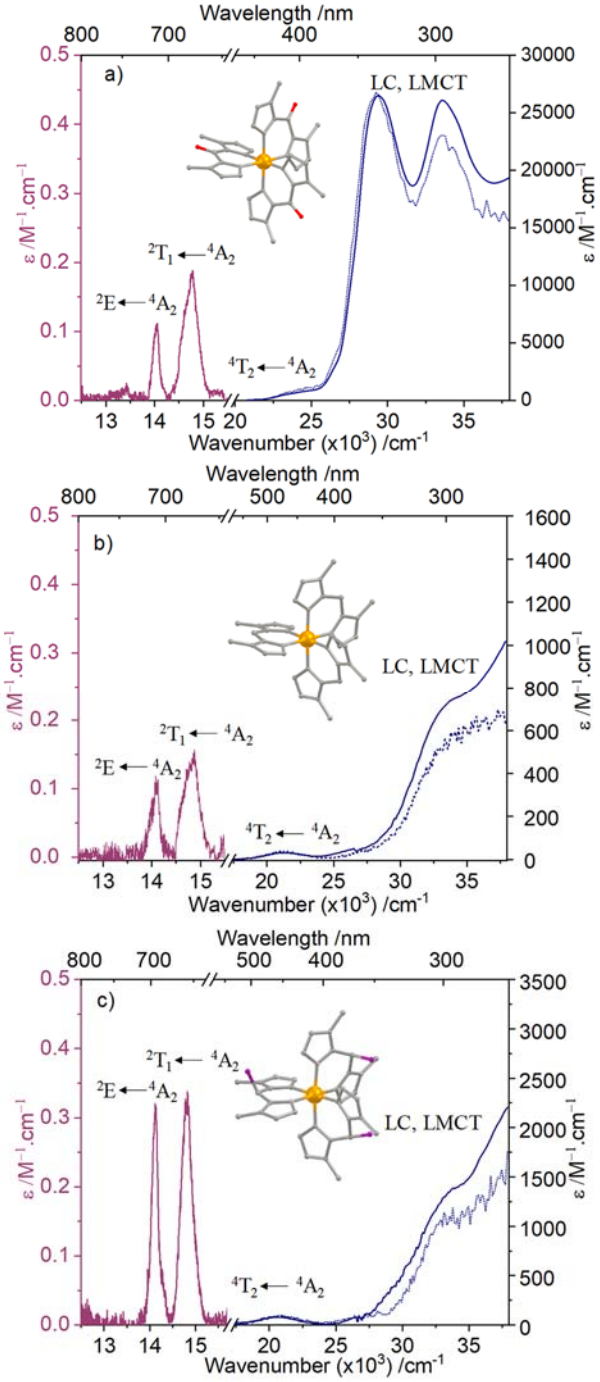

Figure 2. Absorption spectra (full blue traces) in acetonitrile of (a) $[Cr(bik)_3](OTf)_3$ at $3.9x10^{-4}$ M; (b) $[Cr(bim)_3](OTf)_3$ at $4.8x10^{-4}$ M and (c) $[Cr(bie)_3](BF_4)_3$ at $4.0x10^{-4}$ M at 293 K. Excitation

spectra (dotted blue traces) recorded in acetonitrile at 293K with λ_{em}= 710 nm. Absorption spectra centered on spin-flip transitions (purple full traces) recorded in concentrated solutions of (a) $[Cr(bik)_3](OTf)_3$ ($8.1x10^{-3}$ M); (b) $[Cr(bim)_3](OTf)_3$ ($7.7x10^{-3}$ M) and (c) $[Cr(bie)_3](BF_4)_3$ ($4.8x10^{-2}$ M).

The Laporte and spin-forbidden transitions, corresponding to spin-flip $Cr(^2T_1 \leftarrow ^4A_2)$ and $Cr(^2E \leftarrow ^4A_2)$, were observed for the three homoleptic complexes in concentrated media (Figure 2) or in the solid state (Figure S31). Those latter are respectively found at 677 and 712 nm for $[Cr(bik)_3](OTf)_3$, 673 and 709 nm for $[Cr(bim)_3](OTf)_3$; and 674 and 708 nm for $[Cr(bie)_3](BF_4)_3$, with very low molar absorptivity ($\varepsilon < 0.3$ $M^{-1}.cm^{-1}$). Upon excitation into ligand-centered/LMCT bands, the luminescence of the Cr(III) complexes occurs from the lowest- doublet state (^2E) at 77 K, with intense sharp emission bands located 712 nm ($\bar{\nu}$ = 14000 cm^{-1}) for $[Cr(bik)_3](OTf)_3$; 711 nm ($\bar{\nu}$ = 14000 cm^{-1}) for $[Cr(bim)_3](OTf)_3$ and 708 nm ($\bar{\nu}$ = 14100 cm^{-1}) for $[Cr(bie)_3](BF_4)_3$ (Figure 3a-c).[32]

At room temperature, the appearance of a dual emission, visible as shoulders at 679 nm ($\bar{\nu}$ = 14700 cm^{-1}) for $[Cr(bik)_3](OTf)_3$; 675nm ($\bar{\nu}$ = 14800 cm^{-1}) for $[Cr(bim)_3](OTf)_3$ and $[Cr(bie)_3](BF_4)_3$, arises from the thermally-induced population of the $Cr(^2T_1)$ excited-state by its neighboring $Cr(^2E)$ level. All the complexes excitation spectra match well their associated absorption spectra (Figure 2), attesting an efficient population of $^2E/^2T_1$ states through internal conversion after LC/LMCT excitation (Figure 3). The pairs of spin-flip absorption and emission bands are quasi isoenergetic, in other words there is roughly no Stokes shift. These phosphorescence bands are also very narrow as no marked changes in equilibrium bond distances are expected during spin-flip excitation. In addition, to a first order the $Cr(^2T_1 \rightarrow ^4A_2)$ and $Cr(^2E \rightarrow ^4A_2)$ spin-forbidden transitions have no dependency upon Δ (Figure 3d) and are therefore not affected by bandwidth broadening effect that could arise from ligand field strength variations.[33] Yet, it is worth noticing that the spin-flip

emission of these novel tri(didentate) Cr(III) complexes containing 6-membered chelate rings (708 $\leq \lambda_{em}(^2E) \leq$ 712 nm) is slightly blue-shifted with respect to their tri(didentate) counterparts with 5-membered chelate rings, such as $[Cr(phen)_3]^{3+}$(λ_{em} = 728 nm).[16]

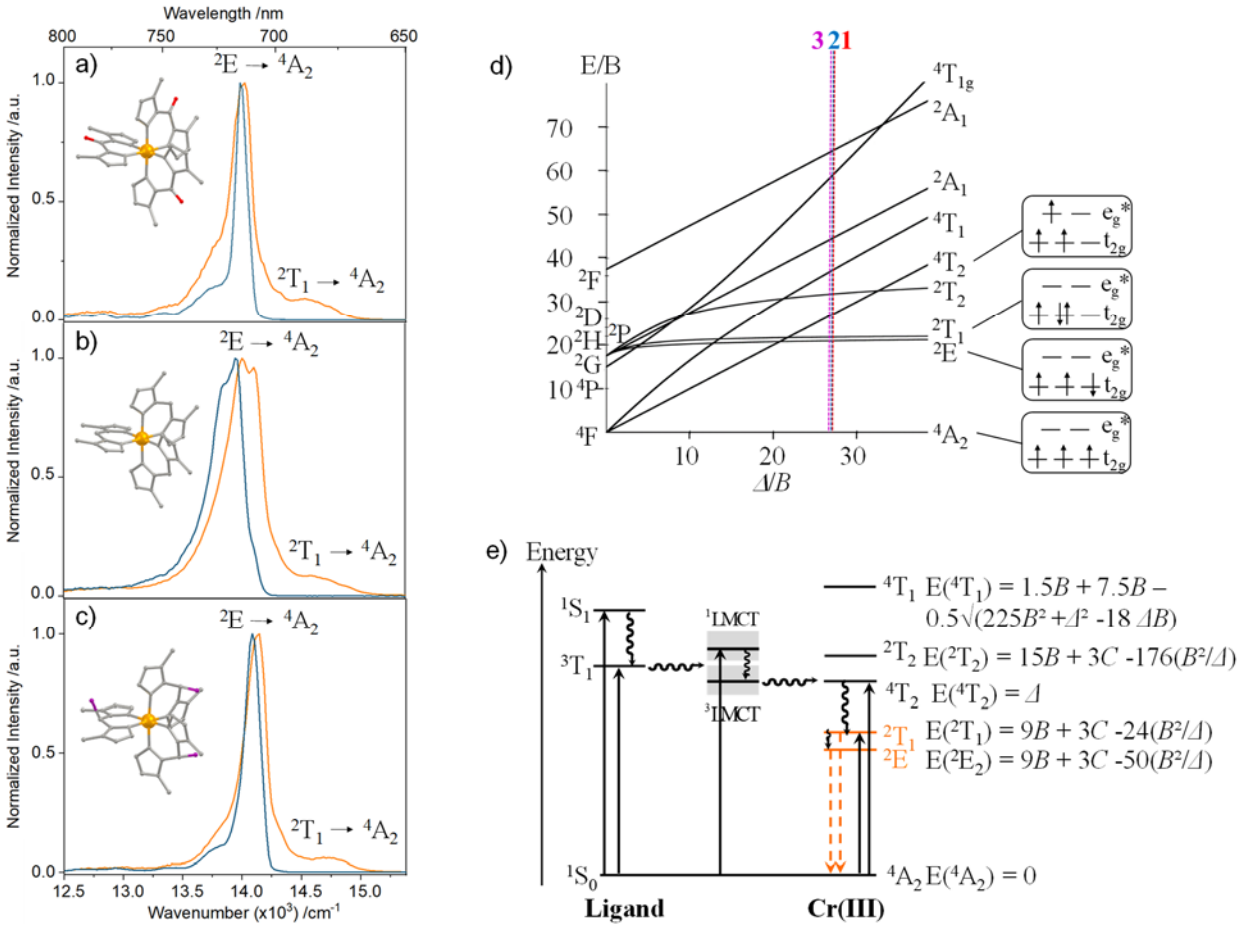

Figure 3. Normalized emission spectra of (a) $[Cr(bik)_3](OTf)_3$, (b) $[Cr(bim)_3](OTf)_3$ and (c) $[Cr(bie)_3](BF_4)_3$ in acetonitrile at 293K (orange traces) and in acetonitrile/propionitrile (6/4) at 77K (blue traces), using λ_{exc} = 340 nm for **1** and **2**, and λ_{exc} = 300 nm for **3**. (d) Tanabe-Sugano diagram for the d^3 configuration in an O_h ligand field highlighting the discussed homoleptic Cr(III) complexes. (e) Schematic energy diagram of $Cr^{III}N_6$ complex in a strong ligand field Δ, illustrating the possible excitation pathways. The energy of metal-centered terms are specified alongside the diagram, as a function of ligand field Δ and Racah parameters (B and C)

The ligand field and Racah parameters were computed (Table 2) using experimental transitions together with the relevant terms and energy expressions given in Figure 3e. It thus follows that Δ

= 23094, 21008 and 20747 cm^{-1} for (**1**), (**2**) and (**3**) respectively, given directly by the Cr($^4T_2 \leftarrow {}^4A_2$) transition energy. Solving for the *B* parameter while assuming $C = 3.5\ B$,[21] provides $804 \geq B \geq 789$ cm^{-1} which decrease in the order (**3**) > (**2**) > (**1**) (Table 2). Compared with bound 5-membered chelate rings as found in $[Cr(phen)_3]^{3+}$ ($\Delta = 22075\ cm^{-1}$, $B = 779\ cm^{-1}$),[21] the larger values of the Racah parameters in the six-membered chelated complexes (**1**)-(**3**) explain the slight blue shift of the Cr($^2E \rightarrow {}^4A_2$) phosphorescence. According to the molecular orbitals of the free ligands bik, bim and bie computed by DFT methods in their optimized geometries (Table S14), one immediately notices that the replacement of the methylene spacer in bim (or a substituted methylene in bie) with a carbonyl unit in bik reduces the HOMO (π-orbital)-LUMO (π*-orbital) gap by approximately 1.5 eV. We therefore observe a significant red-shift of the associated absorption spectrum recorded for the later bik ligand (Figure S30). The second striking difference lies in the higher energy computed for the highest energy σ-orbital in bik (which corresponds to the HOMO-3), compared with bim (HOMO-4) and bie (HOMO-5, Figure S64). A rough analysis thus concludes that one expects a larger ligand-field splitting for $[Cr(bik)_3]^{3+}$, which is indeed detected in its absorption spectrum (Figure 2). Altogether the HOMO and HOMO-1 denote a considerable π-donor character for the three ligands whilst the σ-donating character appeared more pronounced in bik ligand as evidenced by the analysis of the HOMO-3 features. Interestingly, the increase in nephelauxetic effect B(**3**) > B(**2**) > B(**1**), although limited (Table 2), follows the lowering of the energy of the accepting π-orbitals along the series of the pertinent free ligands ($E(\pi^*)$ in Figure S64).

The emitting doublet states lifetimes (τ) were measured in degassed or air-equilibrated acetonitrile solutions at room temperature, and in a glassy acetonitrile/propionitrile mixture (6/4) at 77K (Table 2). All decay curves could be fitted with a mono-exponential function (Figure S32 to S40), with values revealing the following trend τ(**1**) > τ(**2**) > τ(**3**) regardless of the experimental configuration.

At 77K, the three compounds demonstrate exceptionally long millisecond lifetimes, up to 8.2 ms for (**1**). Under ambient conditions, $[Cr(bik)_3](OTf)_3$ and $[Cr(bim)_3](OTf)_3$ lifetimes persist over a hundred of microseconds (τ_{air}=128 µs and 92 µs respectively) while that of $[Cr(bie)_3](BF_4)_3$ drops to a few microseconds (τ_{air} = 8 µs). Several processes may participate in the non-radiative depopulation of the $Cr^{III}(^2E)$ excited-states such as thermally-induced relaxation mechanisms or solvent vibrational modes coupled-quenching mechanisms.[34] In addition, large amplitude trigonal distortions can also act as ^2E excited-state effective quenching channels, a mechanism thoroughly evidenced on a wide range of Cr(III) emitters by Endicott *et al*.[35] Although assessed as the predominant thermal relaxation pathway in most Cr(III) complexes, back-intersystem crossing (BISC) from ^2E to $^4T_2$ state is regarded as limited in complexes **1, 2** and **3,** as their energy gap $\Delta E(^2E\text{-}^4T_2)$ lies above the cut-off value defined by Förster (*i.e*. 3400 cm^{-1}) as the limit for a significant BISC[14] (the lowest being herein 6623 cm^{-1} for $[Cr(bie)_3](BF_4)_3$). Furthermore, the 15-fold difference in τ^{air} for (**3**) with respect to its counterparts (**1** and **2**) is mostly accounted for by supplementary de-activation pathways opened by the presence of C-H (Me_β) oscillators.

Consistently with the short lifetime of its emitting state (^2E and $^2T_1$,), $[Cr(bie)_3](BF_4)_3$ displays the larger ^2E and $^2T_1$ excited states radiative rate constants (k_{rad}) of the series (Table 2). These latter were inferred while integrating spin-flip absorption transitions area (Figure 2) and applying Einstein's equation [36] as follows:

$$k_{\mathrm{rad}} = 2303 \cdot \frac{8\pi c n^2 \bar{\nu}^2 g_{\mathrm{gs}}}{N_{\mathrm{a}} g_{\mathrm{es}}} \int \varepsilon(\bar{\nu})\, d\bar{\nu} \qquad (5)$$

where n is the refractive index of the medium, c is the light velocity, $\bar{\nu}$ is the barycenter of the transition in wavenumbers, N_a is the Avogadro constant, ε is the molar absorption coefficient and g_{gs} and g_{es} are the degeneracy of the ground state and excited-state respectively. For assessing accurately the steady-state emitted intensity (I_i) of the ^2E and $^2T_1$ energy levels, the calculated

radiative rate constants have to be modulated by the normalized excited state population N_i, according to $I_i = k_{\mathrm{rad}}^{i} \cdot N_{\mathrm{i}} = k_{\mathrm{rad}}^{i} \cdot g_i \cdot e^{-\left(\frac{E_i}{k_B T}\right)}$.[37] The intensity ratio $I(^2E)/I(^2T_1)$ can thus be deduced from the energy gap ΔE between the two emitting states, giving: 11, 18 and 16 for (**1**), (**2**) and (**3**) respectively. These values are consistent with the experimental ones found for the three complexes, of 12 for (**1**) and 17 for (**2**) and (**3**). The intrinsic quantum yields of the two ^2E and $^2T_1$ emitting levels could also be determined from equation (6) and are given in Table 2 (entries 9 and 11).

$$\phi_{\mathrm{Cr}}^{i} = k_{\mathrm{rad}}^{i} \cdot \tau_{\mathrm{exp}}^{i} = \frac{k_{\mathrm{rad}}^{i}}{k_{\mathrm{rad}}^{\mathrm{i}} + k_{\mathrm{non-rad}}^{i}} \quad (6)$$

As the two ^2E and $^2T_1$ energy levels are thermally equilibrated at room temperature, a single experimental lifetime value, τ_{exp}, was obtained over the entire wavelength emission range giving $\tau_{exp} = \tau\ (^2E) = \tau\ (^2T_1)$. On this basis, the global non-radiative rate constants were subsequently computed for assessing the non-radiative relaxation processes (Table S9). Furthermore, the sum of the intrinsic quantum yields of the two emitting levels, $\Phi^{\mathrm{intrinsic}} = \Phi_{\mathrm{Cr}}^{^2E} + \Phi_{\mathrm{Cr}}^{^2T_1}$ (Table 2, entries 9 and 12), differ from the overall quantum yield Φ^{tot} obtained upon ligand-centered excitation (λ_{exc} = 450 nm), in aerated and deaerated conditions (Table 2, entries 8 and 11). Knowing that $\Phi^{\mathrm{tot}} = \eta^{\mathrm{sens}} \cdot \Phi^{\mathrm{intrinsic}}$, the sensitization process reaches the $38\% \leq \eta^{\mathrm{sens}} \leq 67\%$ in the $[Cr(\mathbf{L})_3]^{3+}$ complexes (**L** = bik, bim, bie; Table 2, entries 10 and 13). Additionally, the noticeable overall quantum yields observed in the studied series for hexa-coordinated Cr(III) complexes are combined with a limited sensitivity of the intensities and lifetimes $^2E \rightarrow {}^4A_2$ emissions to dioxygen (Table 2). In that sense, $[Cr(bik)_3](OTf)_3$ complex has a longer lifetime (and quantum yield) of only 1.6-fold under dioxygen free atmosphere, while those of $[Cr(bim)_3](OTf)_3$ and $[Cr(bie)_3](BF_4)_3$ are even less sensitive. A similar behavior was reported for the di(tridendate) $[Cr(bpmp)_2]^{3+}$ complex where

bpmp = 2,6-bis(2-pyridyl-methylpyridine).[38] The authors postulated that the anions interacting with the methylene bridges, were shielding the complex from dioxygen quenching. However, the latter proposition would not explain the limited dioxygen sensitivity of the $[Cr(bik)_3](OTf)_3$ which does not possess acidic protons.

Table 2. Ligand field, Racah parameters and photophysical data of $[Cr(\mathbf{L})_3]^{3+}$ complexes (**L** = bik, bim, bie).

Complex	$[Cr(bik)_3]^{3+}$ (**1**)	$[Cr(bim)_3]^{3+}$ (**2**)	$[Cr(bie)_3]^{3+}$ (**3**)
Δ /cm^{-1}	23094	21008	20747
B /cm^{-1}	789	799	804
$k_{rad}(^2E)$[a] /s^{-1}	31	37	60
$k_{rad}(^2T_1)$[b] /s^{-1}	60	58	79
$\tau_{(deae,293K)}$[c] /μs	209	131	7[h]
$\tau_{(Air,293K)}$[d] /μs	128	92	8[h]
$\tau_{(Air,77K)}$[e] /μs	8220	6750	5250
$\Phi^{tot}_{deae,293K}$ [f] /%	0.80	0.47	0.066
$\Phi^{intrinsic}_{deae,293K}$ [f] /%	1.90	1.24	0.111
$\eta^{sens}_{deae,293K}$ [f] /%	42	38	54
$\Phi^{tot}_{air,293K}$ [g] /%	0.47	0.45	0.064
$\Phi^{intrinsic}_{air,293K}$ [g] /%	1.16	0.88	0.111
$\eta^{sens}_{air,293K}$ [g] /%	41	51	58

[a] Computed assuming $C = 3.5\ B$.[21] [b] Radiative decay rates were calculated using equation 5. Experimental lifetimes measured (using λ_{exc}= 355 nm and λ_{em}= 710 nm): [c] under argon atmosphere in freeze-pump thaw degassed acetonitrile at 293 K; [d] air-equilibrated acetonitrile solutions at 293 K; and [e] in acetonitrile/propionitrile (6/4) solutions at 77K in air. Relative

quantum yields, of the overall $Cr^{III}(^2E, {}^2T_1 \rightarrow {}^4A_2)$ emission, were determined using $[Ru(bipy)_3](PF_6)_2$ as standard and performed: [f] under argon atmosphere in freeze-pump-thaw degassed acetonitrile; [g] in air-equilibrated acetonitrile solutions at 293 K, λ_{exc} = 450 nm for all measurements. [h] Note that variation between τ_{air} and τ_{deae} of $[Cr(bie)_3](BF_4)_3$ compound are within the measurement error.

A concomitant and/or alternative hypothesis, suggested in this study, considers the poor overlap between the absorption spectrum of O_2 with the emission spectra of the complexes[39]. This latter aligns with the quenching mechanisms elucidated for $[Cr^{III}(bipy)_3]^{3+}$ complex [40] operating through energy transfer process from the $Cr(^2E)$ excited-state to the ground state triplet $^3O_2$. This finding may apply to other Cr(III) complexes as depicted in Figure S45 (and Table S10) showing an increasing dioxygen insensitivity as their emission maxima deviate from the absorption maximum of O_2 (setting at 760 nm[41]). Finally, one should not loose sight that the dioxygen sensitivity in the general case of Cr(III) complexes depends on multiple parameters whose main(s) contribution(s) may be difficult to elucidate, or to define absolute trends as they appear to be complex-dependent.

Electrochemical study and photooxidant behavior of $[Cr(bik)_3](OTf)_3$.

The electrochemical properties of the complexes were investigated by cyclic voltammetry in acetonitrile containing 0.1 M $TBAPF_6$. Consistently with their spectroscopic data, the 2 x 6 π-electrons $[Cr(bim)_3]^{3+}$ (2) and $[Cr(bie)_3]^{3+}$ (3) complexes did not show any response over the electrochemical window explored. In contrast, the $[Cr(bik)_3]^{3+}$ (1) complex voltammogram revealed three reversible processes at half potential ($\boldsymbol{E^{\circ}_{1/2}}$) of -0.86; -1.18 and -1.40 V respectively (Figure 4, Table 3).

Table 3. Electrochemical data of $[Cr(bik)_3](OTf)_3$ compound (referenced versus ferrocene/ferrocenium) in acetonitrile containing 0.1M $TBAPF_6$.

	Reduction			Oxidation		
	E_{pc}^1	E_{pc}^2	E_{pc}^3	E_{pa}^1	E_{pa}^2	E_{pa}^3
$[Cr(bik)_3]^{3+}$	-0.90	-1.22	-1.44	-0.82	-1.15	-1.36

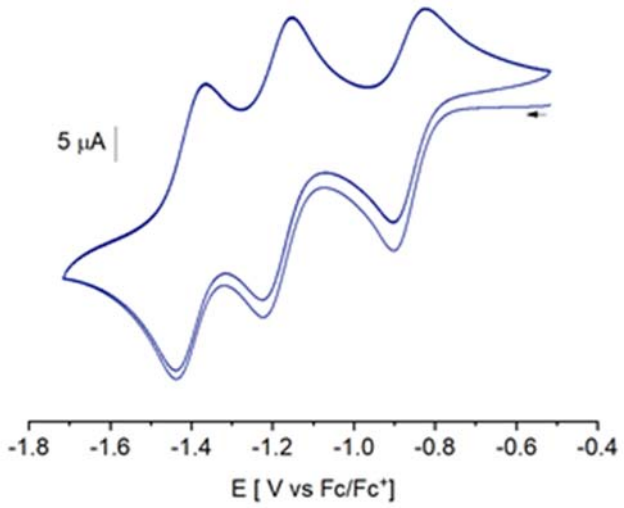

Figure 4. Cyclic voltammogram of $[Cr(bik)_3](OTf)_3$ in acetonitrile (1 mM) with $TBAPF_6$ (0.1 M),with v = 100 $mV \cdot s^{-1}$, at 293 K. The arrow indicates direction of first forward scan.

For further insights into the nature of this redox profile, absorption spectro-electrochemical measurements were carried out (Figure S47) in acetonitrile. The differential absorption spectra, recorded under progressive cathodic potential increments (from -0.46 V to -1.65 V) display mainly ligand-centred spectral changes. Thus, the reductions of $[Cr^{III}(bik)_3]^{3+}$ are clearly ligand orbital-centred events, successively producing the $[Cr^{III}(bik^{\bullet-})(bik)_2]^{2+}$ and $[Cr^{III}(bik^{\bullet-})_2(bik)]^{1+}$ mixed-valence species and $[Cr^{III}(bik^{\bullet-})_3]^0$ final reduced complex. If the free ligand is redox-active and may exist in two different oxidation states (bik^0 and its π-monoradical anion $bik^{\bullet-}$) with $E_{1/2}^{\circ}$ = -2.10 V vs ferrocene (Figure S46), several assets are brought by the coordination to the metal center. Firstly, the reduction potential of bik ligand is anodically shifted upon complex formation, indicating a greater tendency to get reduced. Secondly, although the ligands are chemically equivalent in

$[Cr(bik)_3]^{3+}$ complex, they behave as distinct redox active sites (with different $E^{\circ}_{1/2}$ values). This electrochemical pattern ensues interactions between the sites, supposedly of electrostatic nature, which render the neighbouring reduction a little bit more difficult. It is also worth noting that the ligands calculations are in line with the complexes electrochemical response, as electron transfer occur on the ligands, and illustrate the easier reduction of bik ligand as its LUMO lies at lower energy.

The comproportionation equilibrium constants (K_c) of the mixed-valence complexes calculated from the associated redox potentials differences ($\Delta E^{\circ}_{1/2}$), amount to $3.4x10^5$ for $[Cr^{III}(bik^{\bullet-})(bik)_2]^{2+}$ (eq 7) and $6.4x10^3$ for $[Cr^{III}(bik^{\bullet-})_2(bik)]^{1+}$ (eq 8) species. [42]

$$[Cr^{III}(bik)_3]^{3+} + [Cr^{III}(bik^{\bullet-})_2(bik)]^{1+} \rightleftharpoons 2\,[Cr^{III}(bik^{\bullet-})(bik)_2]^{2+} \quad (7)$$

$$[Cr^{III}(bik^{\bullet-})(bik)_2]^{2+} + [Cr^{III}(bik^{\bullet-})_3]^{0} \rightleftharpoons 2\,[Cr^{III}(bik^{\bullet-})_2(bik)]^{1+} \quad (8)$$

Additionally, when combined with spectroscopic data, the electrochemical description of a Cr(III) complex can provide valuable information on its reactivity, such as the oxidizing power of its ^2E excited state that is given by $E°(*Cr^{III}/Cr^{II})$ value. Such electrochemical and spectroscopic correlations have been mostly underscored with charge-transfer (CT) polypyridyls Ru(II) complexes, [5b),43] whose excited-state reduction potentials could at times be approximated by the following general equation[44]:

$$E°(*X/X^{-}) = E°(X/X^{-}) + \Delta E^{00} \quad (9)$$

where $E°(X/X^{-})$ corresponds to the standard potential of the X/X^{-} redox couple in ground state, and $E°(*X/X^{-})$ to their excited-state reduction potential. ΔE^{00} is energy of the 0-0 transition between X excited and ground states, in eV. This way, Wenger and coworkers[45] recently ascertained the excited-state redox potential of the $[Cr(dqp)_2]^{3+}$ (dqp = 2,6-bis(8′-quinolinyl)pyridine) Cr(III) complex, finding $E°(*[Cr^{III}(dqp)_2]^{3+}/[Cr^{III}(dqp^{\bullet-})(dqp)]^{2+}) = 1.01$ V *vs*

Fc. Applying this principle to $[Cr(bik)_3]^{3+}$ complex gives $E°(*[Cr^{III}(bik)_3]^{3+}/[Cr^{III}(bik^{\bullet-})(bik)_2]^{2+}) = E°([Cr^{III}(bik)_3]^{3+}/[Cr^{III}(bik^{\bullet-})(bik)_2]^{2+}) + \Delta E^{00}$ = 0.89 V (vs Fc; with ΔE^{00} retrieved from the emission spectrum of the compound at 77K in ACN/propionitrile). With $E°(*[Cr^{III}(bik)_3]^{3+}/[Cr^{III}(bik^{\bullet-})(bik)_2]^{2+}) > 0.8$ V (*vs* Fc), the $*[Cr^{III}(bik)_3]^{3+}$species thus belongs to the category of very strong oxidizing agents according to Connelly and Geiger' classification.[46] Also, in comparison with reports of photoelectroactive tri(didentate) Cr(III) counterparts based on 5-membered polypyridyl chelate rings, [47] complex **(1)** lies in the lower range of the excited-state oxidants nearby the homoleptic $[Cr(phen)_3]^{3+}$ and $[Cr(bipy)_3]^{3+}$(1.05 V and 1.08 vs Fc/Fc^+ respectively).

Therefore, partnering redox non-innocent ligands with Cr(III) metal center can give rise to mononuclear complexes with electrochemical pattern as rich as the polymetallic complexes ones, such as Prussian Blue Analogues or polyoxometalates.[47] The ^{2}E excited-state strong oxidizing power of the Cr(III) complexes is also gaining more attention over ^{3}MLCT excited-state Ru(II)-based photooxidants, in photocatalysis.[48]

Acido-basic properties of the β-diketimines derivatives.

On their side, the $[Cr(bim)_3](OTf)_3$ and $[Cr(bie)_3](BF_4)_3$ complexes present a different kind of attractive feature, imparted by the *Brønsted-Lowry* acid character of the bim and bie ligands. Those latter possess a β-diketimine motif, reminiscent of the well-known β-diketone moiety, which consequently have acidic α- hydrogens. In their anionic form, *i.e* β-diketiminates, the π-electron system is delocalized over the whole structure (the same applies to their enamine tautomers, when they exist).

A first evidence of the above-mentioned acidic features lies in hydrogen bonds between the aliphatic bridges and the anions, observed in both $[Cr(bim)_3](OTf)_3$ and $[Cr(bie)_3](BF_4)_3$ complexes

crystalline packing (Figure 5). In $[Cr(bim)_3](OTf)_3$ complex, CH···O distances between methylene bridges and triflate anions span the range of 2.27-2.59Å (ΣVan der Waals radii = 2.62Å), over the three different crystallographic sites, and $\widehat{CH\cdots O}$ angles are found between 129-138°. For the $[Cr(bie)_3](BF_4)_3$ complex, hydrogens bonds are present at a distance mean value of 2.45Å between the C-H bridges and BF_4^- anions (ΣVdW radii = 2.57Å) and $\widehat{CH\cdots F}$ angles covering the interval 109-173°.

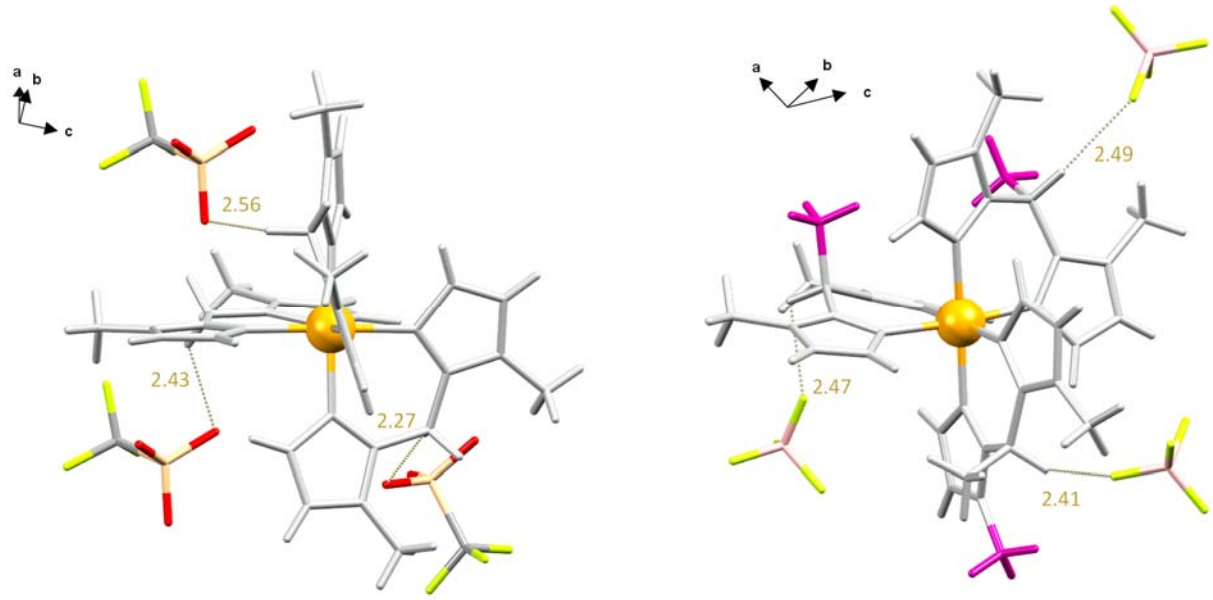

Figure 5. Perspective views of $[Cr(bim)_3](OTf)_3$ (left) and $[Cr(bie)_3](BF_4)_3$ (right) showing C-H··anions interactions. Cr atoms are shown in orange, the rest of the complexes structure is displayed in grey (except the Meβ in *C*1-symmetrical $[Cr(bie)_3]^{3+}$ highlighted in violet).

The influence of the acid-base properties of $[Cr(bim)_3](OTf)_3$ and $[Cr(bie)_3](BF_4)_3$ complexes on their emissive properties were investigated in acetonitrile solution. For instance, deprotonation of the $[Cr(bim)_3](OTf)_3$ methylene bridges by sequential additions of *N*,*N*-diisopropylethylamine (DIPEA) leads to a color change of the solution, from orange to blue, accompanied by a decrease of the emission at 710 nm (Figure 6). The luminescence of the complex was 78% recovered following the addition of 3 eq of triflic acid. The incomplete nature of this luminescence 'ON-OFF'

process is presumably due to the propensity of the bis(heteroaryl)methanes (and relatives) to oxidize. A similar incomplete pattern was observed (Figure S48) for the deprotonation/protonation studies of $[Cr(bie)_3](BF_4)_3$ complex, which required the use of the stronger base, DBU (1,8-diazabicyclo[5.4.0]undec-7-ene).

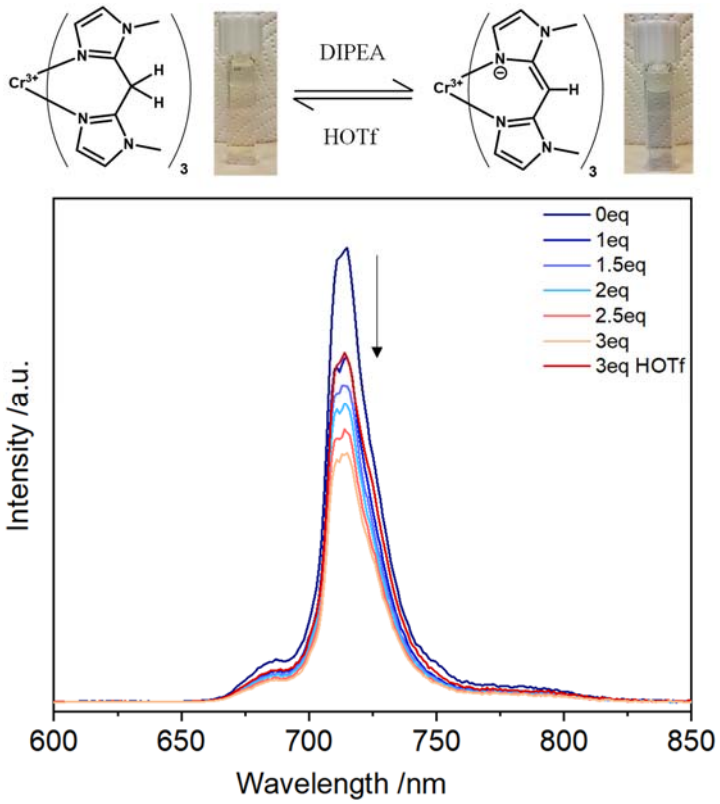

Figure 6. Intensity of the $[Cr(bim)_3](OTf)_3$ emission band along the deprotonation-protonation cycle (*i.e.* successive additions of DIPEA followed by 3eq of HOTF).

As pointed out in several reports, this β-diketimine compounds family can undergo spontaneous oxidation in the presence of water or even metal-catalyzed oxidation in the presence of dioxygen[49] The reaction leads to the formation of their ketone equivalents involving the NH/CH tautomeric equilibrium of the considered derivative. Furthermore, the LRMS analysis of a basic $[Cr(bim)_3](OTf)_3$ acetonitrile solution evolving in air for half an hour, displayed the signals pattern than the oxidized mixture in Figure S17. Notwithstanding our efforts to work in deaerated and anhydrous media, we could not fully prevent these side reactions owing notably to the constant

amount of residual water in acetonitrile that could not be reduced below 20 ppm.[50] These findings nevertheless revealed the stability of the $[Cr(bim)_3](OTf)_3$ and $[Cr(bie)_3](BF_4)_3$ complexes regarding degradation in basic media, following hydroxo anions substitutions. These studies also open an interesting possible scope of investigations on the reversibility of these oxidation processes and the resulting chemistry-on-Cr(III) complexes, which remains to date scarcely reported.

Conclusion

The synthesis of the first polyaromatic homoleptic tri(didentate) Cr(III) complexes with 6-membered chelate rings was successfully unlocked using the bis(imidazolyl)-chelates: bik, bim and bie. Detailed thermodynamic and theoretical studies unraveled the origin of the quantitative formation of the C_1-symmetrical $[Cr(bie)_3](BF_4)_3$ whose isomeric ratio is biased by intramolecular interligand interactions. The 6-membered chelate rings formed by the three ligands, embed the Cr(III) ion in a strong ligand-field and a $\{Cr^{III}N_6\}$ micro-symmetry close to the ideal octahedron. This offers a favorable configuration for the observation of the NIR-luminescence of the three complexes. The key photophysical parameters of the three homoleptic complexes (*i.e*. excited-state lifetimes, overall phosphorescence quantum yield) rank in the upper part of the tri(didentate) Cr(III) complexes category. The position of their blue-shifted $Cr^{III}(^2E, {}^2T_1 \rightarrow {}^4A_2)$ emission band, located at *ca*. 710 nm, enabled a better understanding of the design of dioxygen insensitive Cr(III) emitters, owing to the poor overlap with the oxygen absorption spectrum. Beyond the general improvement of the photophysical features, partnering the Cr(III) ion with the redox non-innocent ligand bik or the β-diketiminate ligands bim and bie provides an innovative set of switchable properties. The $[Cr(bik)_3](OTf)_3$ complex behaves as a multi-electron reservoir with an interesting photooxidant behavior, both combined are of potential interest for different types of applications as photocharge accumulation[47b),51] or photocatalysis[48]. On their side, the $[Cr(bim)_3](OTf)_3$ and $[Cr(bie)_3](BF_4)_3$

complexes acidic features afforded a useful understanding for the design of chemo-switches Cr(III) complexes whose general interest spans diverse research fields such as bioimaging, colorimetric sensors or even more generally multifunctional molecular materials science. Finally, one notes that the negligible electronic effects accompanying the switch from 2 x 6 π-electrons to 14 π-electrons in going from bipy to phen for polyaromatic 5-membered rings, is not strictly mirrored for related 6-membered rings in going from bim to bik. Indeed, the electronic absorption spectra, ligand-field and Racah parameters computed in the $[Cr\mathbf{L}_3]^{3+}$ complexes reflect the combination of (i) the electron-withdrawing character of the additional oxygen atom with (ii) the improved potential π-delocalization with bound bik units, which make $[Cr(bik)_3]^{3+}$ quite different from $[Cr(bim)_3]^{3+}$.

ASSOCIATED CONTENT

Supporting Information. The supporting information is available free of charge on the ACS publication website at DOI:

Experimental details; syntheses; NMR, HRMS, IR characterizations; symmetry number method; XRD analyses; Photophysical measurements; Cyclic voltammetry measurements; Acid-base properties; theoretical studies (PDF).

AUTHOR INFORMATION

Corresponding Author

*Email : amina.benchohra@unige.ch

*Email: claude.piguet@unige.ch

Present Addresses

†A.B.: Laboratoire CEMCA- UMR, CNRS 6521. UFR Sciences & Techniques, 6 avenue Victor Le Gorgeu 29238 BREST CEDEX 3, France. Email : amina.benchohra@univ-brest.fr; C.M.C : Department of Organic Chemistry, Unidad de Excelencia de Química (UEQ) University of Granada, Avda. Fuente Nueva.

Author Contributions

The manuscript was written through contributions of all authors. All authors have given approval to the final version of the manuscript.

Funding Sources

This work was supported through grants from the Swiss National Science Foundation (grant 200020_207313).

ORCID :

Amina Benchohra: 0000-0002-6060-6894; Julien Chong: 0000-0003-4916-6899; Carlos Moreno Cruz : 0000-0002-0676-5210 ; Céline Besnard : 0000-0001-5699-9675 ; Arnulf Rosspeintner : 0000-0002-1828-5206 ; Claude Piguet : 0000-0001-7064-8548.

ACKNOWLEDGMENT

The authors gratefully thank Dr A. Fürstenberg for helpful advice as well as Dr C. Larsen for discussions and the $[Ru(bipy)_3](PF_6)_2$ supply. We also gratefully thank K. L Paglia for elemental analyses and the HRMS MZ 2.0 core facility, in particular Dr E. Varesio and Mr. H. Théraulaz, for their assistance with mass spectrometry measurements. We gratefully thank Prof. Lescouëzec and the Pôle 2 of the Institut Parisien de Chimie Moléculaire (IPCM) for providing us access to absorption spectro-electrochemical material. This work made use of the infrastructure services

provided by S3IT (www.s3it.uzh.ch), the Service and Support for Science IT team at the University of Zurich. The authors would like to thank the S3IT team for their support. The authors thank the Centro de Servicios de Informática y Redes de Comunicación (CSIRC), Universidad de Granada, for providing the computing time.

Conflict of interest

The authors declare no conflict of interest.

REFERENCES

[1] a) Schwarzenbach, G.; Der Chelateffekt. *Helv. Chim. Acta* **1952**, *35*, 39.-65.b) Martell, A. E.; The chelate effect. *Adv. Chem. Ser.* **1967**, *62*, 272-294.

[2] a) Schwarzenbach, G.; Flaschka, H.; Complexometric Titrations, United Kingdom, Methuen; 2nd edition, **1969**; b) Guerriero, P.; Tamburini, S.; Vigato, P. A.; From mononuclear to polynuclear macrocyclic or macroacyclic complexes. *Coord. Chem. Rev.* **1995**, *139*, 17-243.

[3] a) Hancock, R. D.; Martell, A. E.; Ligand design for selective complexation of metal ions in aqueous solution. *Chem. Rev.* **1989**, *89*, 1875-1914; b) Martell, A. E.; Hancock, R. D.; Motekaitis, R. J.; Factors affecting stabilities of chelate, macrocyclic and macrobicyclic complexes in solution. *Coord. Chem. Rev.* **1994**, *133*, 39-65; c) Hancock, R. D.; Nikolayenko, I. V.; Do Nonbonded H--H Interactions in Phenanthrene Stabilize It Relative to Anthracene? A Possible Resolution to this Question and Its Implications for Ligands such as 2,2′-Bipyridyl; *J. Phys. Chem. A* **2012**, *116*, 8572-8583.

[4] Smith, R. M.; Martell, A. E.; *Critical Stability Constants, Inorganic Complexes*, Springer New York, NY, **2013**.

[5] a) Meyer, T. J.; Photochemistry of metal coordination complexes : metal to ligand charge transfer excited states. *Pure Appl. Chem.* **1986**, *58*, 1193-1206; b) Endicott, J. F.; Schlegel, H. B.; Uddin, M. J.; Seniveratne, D. S.; MLCT excited states and charge delocalization in some ruthenium-ammine-polypyridyl complexes. *Coord. Chem. Rev.* **2002**, *229*, 95-106.

[6] Zare, D.; Piguet, C.; Prescimone, A.; Housecroft, C. E.; Constable, E. C.; Positive Cooperativity Induced by Interstrand Interactions in Silver(I) Complexes with α,α′-Diimine Ligands. *Chem. Eur. J.* **2022**, *28*, e202200912.

[7] a) Clar, E.; *The Aromatic Sextet*, John Wiley & Sons LTD, London, New York, Sydney, Toronto 1972; b) Sola, M.; Forty years of Clar's aromatic π-sextet rule. *Front. Chem.* **2013**, 1, ARTN22.

[8] Solà, M.; Boldyrev, A. I.; Cryanski, M. K.; Krygowski, T. M.; Merino, G.; *Aromaticity and Antiaromaticity*, John Wiley ¬ Sons Ltd., Chichester, pp 11.

[9] Byers, P. K.; Canty, A. J.; Engelhardt, L. M.; Patrick, J. M.; White, A. H.; Co-ordination chemistry of pyridyl and N-methylimidazolyl ketones. Synthetic and X-ray structural studies of copper(II), nickel(II), and dimethylgold(III) complexes. *J. Chem. Soc. Dalton Trans.* **1985**, 981-986.

[10] a) Bousseksou, A.; Place, C.; Linares, J.; Varret, F.; Dynamic spin crossover in [Fe(2-BIK)$_3$](ClO$_4$)$_2$ and [Fe(Me$_2$2-BIK)$_3$](BF$_4$)$_2$ investigated by Mössbauer spectroscopy. *J. Magn. Magn. Mater.* **1992**, *104*, 225-226; b) Grhel, M.; Krebs, B.; Reaction of Model Nucleobases with the Diaqua(bis(N-methylimidazol-2-yl) ketone)platinum(II) Dication. Synthesis and Structure of the Head-to-Tail Isomers of Bis(9-methylguanine-N7)(bis(N-methylimidazol-2-yl) ketone)platinum(II) Perchlorate, Bis(1-methylcytosine-N3)(bis(N-methylimidazol-2-yl) ketone)platinum(II) Perchlorate, Bis(.mu.-1-methylthyminato-N3,O4)bis[(bis(N-methylimidazol-2-yl) ketone)platinum(II)] Perchlorate, and Bis(.mu.-1-methyluracilato-N3,O4)bis[(bis(N-methylimidazol-2-yl) ketone)platinum(II)] Nitrate. *Inorg. Chem.* **1994**, *33*, 3877-3885; c) Chen, X. M.; Xu, Z. T.; Mak, T. C. W.; Synthesis of bis(N-methylimidazol-2-yl)ketone (BIK) and crystal structure of [Zn(BIK)$_2$](ClO$_4$)$_2$. *Polyhedron* **1995**, *14*, 319-322; d) Stange, A. F.; Kaim, W.; Bis(homoleptische) vs. heteroleptische Kupfer(I)-Komplexe: Elektrosynthese, Spektroskopie und Kristallstruktur von {[Cu(BIK)$_2$]$^+$}$_2${[Cu$_4$(SR)$_6$]$^{2-}$}·3(CH$_3$CN) (RSH); BIK = Bis(N-methylimidazol-2-yl)keton, R = o-Tolyl. *Z. Anorg. Allg. Chem.* **1996**, *622*, 1118-11124; e) Elgafi, S.; Field,

L. D.; Messerle, B. A; Hambley, T. W.; Turner, P.; Synthesis of novel ruthenium complexes containing bidentate imidazole-based ligands. *J. Chem. Soc. Dalton Trans.* **1997**, 2341-2346; f) Elgafi, S.; Field, L. D.; Messerle, B. A.; Turner, P.; Hambley, T. W.; Rhodium complexes containing bidentate imidazolyl ligands: Synthesis and structure. *J. Organomet. Chem.* **1999**, *588*, 69-77; g) Hornung, F. M.; Heilmann, O.; Kaim, W.; Zalis, S.; Fiedler, J.; Metal vs Ligand Reduction in Complexes of 1,3-Dimethylalloxazine (DMA) with Copper(I), Ruthenium(II), and Tungsten(VI). Crystal Structures of (DMA)WO_2Cl_2 and (Bis(1-methylimidazol-2-yl)ketone)WO_2Cl_2. *Inorg. Chem.* **2000**, *39*, 4052-4958; h) Braussaud, N.; Ruther, T.; Cavell, K. J.; Skelton, B. W.; White, A. H.; Bridged 1-Methylbisimidazoles as Building Blocks for Mixed Donor Bi- and Tridentate Chelating Ligands. *Synthesis* **2001**, 626-632.

[11] De, S.; Tewary, S.; Garnier, D.; Li,Y.; Gontard, G.; Lisnard, L.; Flambard, A.; Breher, F. Boillot, M.L.; Rajaraman, G.; Lescouëzec, R.; Solution and Solid-State Study of the Spin-Crossover $[Fe^{II}(R\text{-bik})_3](BF_4)_2$ Complexes (R = Me, Et, Vinyl)*Eur. J. Inorg. Chem.* **2018**, 414-428.

[12] a) Kitzmann, W.R.; Heinze, K.; Charge-Transfer and Spin-Flip States: Thriving as Complements. *Angew. Chem. Int. Ed.*, **2022**, e202213207; b) Scattergood, P.A.; Recent advances in coordination chemistry: luminescent materials and photocatalysis. *Organomet. Chem*, **2021**, 43, 1-34; c) Büldt, L. A.; Wenger, O. S.; Chromium complexes for luminescence, solar cells, photoredox catalysis, upconversion, and phototriggered NO release. *Chem. Sci.* **2017**, *8*, 7359-7367; d) Kandasamy, B.; Ramar, G.; Zhou, L.; Han, S.T.; Venkatesh, S.; Cheng, S.-C.; Xu, Z.; Ko, C.C.; Roy, V. A. L.; Polypyridyl chromium(III) complexes for non-volatile memory application: impact of the coordination sphere on memory device performance. *J. Mater. Chem. C*, **2018**,6, 1445-1450.

[13] a) Otto, S.; Grabolle, M.; Förtser, C.; Kreitner, C.; Resh-Genger, U.; Heinze, K.; $[Cr(ddpd)_2]^{3+}$: A Molecular, Water-Soluble, Highly NIR-Emissive Ruby Analogue. *Angew. Chem. Int. Ed.*, **2015**, 54, 11572-11576 ; b) Jiménez, J.-R.; Doistau, B.; Cruz, C. M.; Besnard, C.; Cuerva, J. M.; Campaña, A. G.; Piguet, C.; Chiral Molecular Ruby $[Cr(dqp)_2]^{3+}$ with Long-Lived Circularly Polarized Luminescence. *J. Am. Chem. Soc*., **2019**, 141, 13244-1252; c) Sinha, N.; Jiménez, J.R.; Pfund, B.; Prescimone, A.C. ; Piguet, C.; Wenger, O.S. ; A Near-Infrared-II Emissive Chromium(III) Complex. *Angew. Chem. Int. Ed.,* **2021**, 60, 23722-23728.

[14] a) Forster, L. S.; The photophysics of chromium(III) complexes. *Chem. Rev*. **1990**, 90, 331-353; b) Forster, L. S.; Thermal relaxation in excited electronic states of d^3 and d^6 metal complexes*. Coord. Chem. Rev*. **2002**, 227, 59-92; c) Fucaloro, A. F.; Forster, L. S.; Rund, J. V.; Lin, S. H.; 2E relaxation in mixed-ligand $Cr(NH_3)_6$-nXn complexes *J. Phys. Chem*., **1983**, 87, 1796-1799.

[15] a) Serpone, N.; Jamieson, M.A.; Henry, M.S.; Hoffman, M.Z.; Bolletta, F.; Maestri, M.; Excited-state behavior of polypyridyl complexes of chromium(III). *J. Am.Chem. Soc.*, **1979**, 101, 2907-2916. b) McDaniel, A.M.; Tseng, H.-W.; Damrauer, N.H.; Shores, M.P.; Synthesis and Solution Phase Characterization of Strongly Photooxidizing Heteroleptic Cr(III) Tris-Dipyridyl Complexes. *Inorg. Chem*., **2010**, 49, 7981-7991.

[16] Otto, S.; Dorn, M.; Förster, C.; Bauer, M.; Seitz, M.; Heinze, K.; Understanding and exploiting long-lived near-infrared emission of a molecular ruby. *Coord. Chem Rev*., **2018**, 359, 102-111.

[17] Wang, C.; Kitzmann, W.R.; Weigert, F.; Förster, C.; Wang, X.; Heinze, K.; Resch-Genger , U.; Matrix Effects on Photoluminescence and Oxygen Sensitivity of a Molecular Ruby. *ChemPhotoChem*, **2022**, e202100296.

[18] a) Sinha, N.; Yaltseva, P.; Wenger, O.S.; The Nephelauxetic Effect Becomes an Important Design Factor for Photoactive First-Row Transition Metal Complexes. *Angew. Chem. Int. Ed.* **2023**, 62, e202303864; b) Cheng, Y.; Yang, Q.; He, J.; Zou, W.; Liao, K.; Chang, X.; Zou, C.; Lu, W.; The energy gap law for NIR-phosphorescent Cr(III) complexes. *Dalton Trans.* **2023**, 52, 2561-2565; c) Sawicka, N.; Craze, C.J.; Horton, P.N.; Coles, S.J.; Richards, E.; Pope, S.J.A.; Long-lived, near-IR emission from Cr(III) under ambient conditions. *Chem. Commun.* **2022**, 58, 5733-5736; d) Stein, L.; Boden, P.; Naumann, R.; Forster, C.; Niedner-Schatteburg, G.; Heinze, K.; The overlooked NIR luminescence of $Cr(ppy)_3$. *Chem. Commun.* **2022**, 58, 3701-3704; e) Kitzmann, W. R.; Moll, J.; Heinze, K.; Spin-flip luminescence. *Photoch. Photobio. Sci.* **2022**, 21, 1309-1331; f) Treiling, S.; Wang, C.F.; Förster, C.; Reichenauer, F.; Kalmbach, J.; Boden, P.; Harris, J.P.; Carrella, L.; Rentschler, E.; Resch-Genger, U.; Reber, C.; Seitz, M.; Gerhards, M.; Heinze, K.; Luminescence and Light-Driven Energy and Electron Transfer from an Exceptionally Long-Lived Excited State of a Non-Innocent Chromium(III) Complex. *Angew. Chem. Int. Ed.* **2019**, 58, 18075-18085.

[19] a) Hawkins, C.J.; *Absolute configuration of metal complexes*, Wiley-Interscience, NewYork, **1971**; b) Jurnak, F.A.; Raymond, K. N.; Conformations of Six-Membered Rings in Tris Metal Complexes. A Skew-Boat Conformation in $[Cr(NH_2CH_2CH_2CH_2NH_2)_3]^{3+}$. *Inorg. Chem*. **1972**, 11, 12, 3149-3152; c) Kaizaki, S.; Hidaka, J.; Shimura, Y.; Circular dichroism of chromium(III) complexes. IV. Elucidation of circular dichroism in the spin-forbidden transitions. *Inorg. Chem*., **1973**, 12, 142-150.

[20] a) Zare, D.; Doistau, B.; Nozary, H.; Besnard, C.; Guénée, L.; Suffren, Y.; Pelé, A.-L.; Hauser, A.; Piguet, C.; Cr^{III} as an alternative to Ru^{II} in metallo-supramolecular chemistry. *Dalton Trans*., **2017**, 46, 8992-9009; b) Barker, K.D.; Barnett, K. A.; Connell, S.M.;

Glaeser, J.W.; Wallace, A.J.; Wildsmith, J.; Herbert, B.J.; Wheeler, J.F.; Kane-Maguire, N.A.P.; Synthesis and characterization of heteroleptic $Cr(diimine)_3^{3+}$ complexes. *Inorg. Chim. Acta*, **2001**, *316*, 41-49; c) Schönle, J.; Constable, E.C.; Housecroft, C.E.; Neuburger, M.; Zampese, J.A.; Heteroleptic chromium(III) tris(diimine) $[Cr(N^N)_2(N'^N')]^{3+}$ complexes *Inorg. Chem. Comm*., **2015**, 51,75-77; d) Kirk, A.D.; Photochemistry and Photophysics of Chromium(III) complexes. *Chem. Rev.*, **1999**, 6, 1607-1640.

[21] Doistau, B.; Collet, G.; Acuña Bolomey, E.; Sadat-Noorbakhsh, V.; Besnard, C.; Piguet, C.; Heteroleptic Ter-Bidentate Cr(III) Complexes as Tunable Optical Sensitizers. *Inorg. Chem*. **2018**, 57, 22, 14362-14373.

[22] a) Rüther, T.; Cavell, K. J.; Braussaud, N. C.; Skelton, B. W.; White, A.H.; Synthesis, characterisation and catalytic behaviour of a novel class of chromium(III) and vanadium(III) complexes containing bi- and tri-dentate imidazole chelating ligands: a comparative study. *J. Chem. Soc., Dalton Trans*., **2002**, 4684-4693. b) Rüther, T.; Braussaud, N.; Cavell, K.J.; Novel chromium (III) complexes Containing Imidazole-Based Chelate Ligands with Varying Donor Sets: Synthesis and Reactivity. *Organom*., **2001**, 20, 1247-1250.

[23] a) Braussaud, N.; Rüther, T.; Cavell, K.J.; Skelton, B.W.; White, A.H.; Bridged 1-Methylbisimidazoles as Building Blocks for Mixed Donor Bi- and Tridentate Chelating Ligands. *Synthesis*, **2001**, 4, 626-632. b) Burling, S.; Field, L.D.; Messerle, B.A.; Rumble, S.L.; Late Transition Metal Catalyzed Intramolecular Hydroamination: The Effect of Ligand and Substrate Structure. *Organom*., **2007**, 26, 4335-4343.

[24] Cantuel, M.; Bernardinelli, G.; Imbert, D.; Bünzli, J.-C. G.; Hopfgartner, G.; Piguet, C.; A kinetically inert and optically active Cr^{III} partner in thermodynamically self-assembled heterodimetallic non-covalent d–f podates. *J. Chem. Soc., Dalton Trans*. **2002**, 1929-1940.

[25] Cotton, F.A.; Wilkinson, G.; *Advanced Inorganic Chemistry*, J. Wiley & sons, **1976**.

[26] The ligand coordination to the metal can proceed in two ways that can be defined as clockwise (C) and anticlockwise (A), with a probability of 1/2 each. If the binding events are considered independent, the arrangement of three bie ligands around the metal leads to 8 possible outcomes, each of a probability of 1/8. Thus, the probability of having all ligands in same direction (or having C_3 symmetrical isomer) is 2/8 (AAA and CCC combinations) while the one of having ligands in mixed directions (or C_1-symmetrical isomer) is 6/8.

[27] Benson, S.W.; Statistical Factors in the Correlation of Rate Constants and Equilibrium Constants. *J. Am. Chem. Soc*. **1958**, 80, 19, 5151-5154.

[28] a) Ercolani, G.; Assessment of cooperativity in self-assembly. *J. Am. Chem. Soc*. **2003**, 125, 51, 16097-16103. b) Ercolani, G.; Piguet, C.; Borkovec, M.; Ha-macek, J.; Symmetry Numbers and Statistical Factors in Self-Assembly and Multivalency. *J Phys Chem B*., **2007**, 111, 12195-12203. c) Piguet, C.; Five thermodynamic describers for addressing serendipity in the self-assembly of polynuclear complexes in solution. *Chem. Commun*, **2010**, 14, 46, 6209-6231.

[29] a) Hamacek, J.; Borkovec, M.; Piguet, C.; Simple thermodynamics for unravelling sophisticated self-assembly processes. *Dalt. Trans.*, **2006**, 1473-1490. b) Piguet, C.; *Handbook on the Physics and Chemistry of Rare Earths*, Elsevier Science, **2015**; 47, 209-271.

[30] Guionneau, P. ; Marchivie, M. ; Bravic, G. ; Létard, J.-F. ; Chasseau, D. ; Structural aspects of Spin Crossover. example of the $[Fe^{II}L_n(NCS)_2]$ complexes. *Top Curr Chem*, **2004**, 234, 97-128.

[31] a) Webb, C.E.; Jones, J.D.C.; *Handbook of Laser Technology*, IOP Publishing Ltd, **2004**. b) Ballhausen, C.J.; *Introduction to ligand field theory*, McGraw-Hill Book company, **1962**.

[32] The energetic order of the $^2E/^2T_1$ is assumed to follow the Tanabe-Sugano diagram shown in Figure 3d and established for pure octahedral symmetry. We are aware that an inverted ordering was recently reported for $[Cr(ddpd)_2]^{3+}$. Kitzmann, W. R.; Ramanan, C.; Naumann, R.; Heinze, K.; Molecular ruby: exploring the excited state landscape. *Dalton Trans.* **2022**, 51, 6519-6525.

[33] Lever, A.B.P.; *Inorganic Electronic Spectroscopy*, Elsevier, **1984**.

[34] Bünzli J.C. and Chopin, G.; *Lanthanide probes in life, chemical and earth sciences: Theory and practice,* Elsevier, **1989**.

[35] a) Endicott, J. F.; Perkovic, M. W.; Heeg, M.J; Ryu, C.K.; Thompson, D.; Ligand-Induced, Stereochemical Relaxation of Electronic Constraints in a Simple Chemical Process. *Adv. Chem*., **1997**, 253, 199-220. b) Endicott, J. F.; Ryu, C.K.; Lessard, R.B.; Hoggard, P.E.; *Photochemistry and photophysics of coordination compounds*, Springer,**1987**.

[36] a) Strickler, S. J.; Berg, R.A.; Relationship between Absorption Intensity and Fluorescence Lifetime of Molecules. *J. Chem, Phys*., **1962**, 37, 814-822; b) Birks, J.B.; Dyson, D.J.; The relations between the fluorescence and absorption properties of organic molecules. *Proc.Roy.Soc. A*, **1963**, 275, 135-148.

[37] a) Suffren, Y.; Zare, D.; Eliseeva, S.V.; Guénée, L.; Nozary, H.; Lathion, T.; Aboshyan-Sorgho, L.; Petoud, S.; Hauser, A.; Piguet, C.; Near-Infrared to Visible Light-Upconversion in Molecules: From Dream to Reality. *J. Phys. Chem. C,* **2013**, 117, 26957-26963.

[38] Reichenauer, F.; Wang, C.; Förster, C.; Boden; P.; Ugur, N.; Báez-Cruz, R.; Kalmbach, J.; Carella, L. M.; Rentschler, E.; Ramanan, C.; Niedner-Schatteburg, G.; Gerhards, M.; Seitz, M.; Resch-Genger, U.; Heinze. K.; Strongly Red-Emissive Molecular Ruby $[Cr(bpmp)_2]^{3+}$ Surpasses $[Ru(bpy)_3]^{2+}$**.** *J. Am. Chem. Soc*., **2021**, 143, 11843-11855.

[39] Jockusch, S.; Turro, N. J.; Thompson, E. K.; Gouterman, M.; Callis, J. B.; Khalil, G. E.; Singlet molecular oxygen by direct excitation. *Photoch. Photobio. Sci.*, **2008**, 7, 235-239.

[40] Tiyabhorn, A.; Zahie, K.O.; Quantum yield of singlet dioxygen and elucidation of the quenching mechanism for the reaction between the doublet excited states of tris(bipyridine)chromium(III) and triplet dioxygen. *Can. J. Chem*. **1996**, 74, 336-340.

[41] Bregnhøj, M.; McLoughlin, C. K.; Breitenbach, T.; Ogilby, P.R.; $X^3\Sigma_g^- \rightarrow b^1\Sigma_g^+$ Absorption Spectra of Molecular Oxygen in Liquid Organic Solvents at Atmospheric Pressure. *J. Phys. Chem. A*, **2022**, 126, 3839-3845.

[42] Launay, J.P.; Verdaguer M.; *Electrons in Molecules*, Oxford, **2018**.

[43] Dodsworth, E.; Lever, A.B.P.; Correlations between electrochemical potentials and optical charge transfer energies in ruthenium bipyridine derivatives. *Chem. Phys. Lett.*, **1986**, 124, 152-158.

[44] Leonhardt, H.; Weller, A.; Elektronenubertragungsreaktionen angeregten perylens. *Berichte Der Bunsengesellschaft Für Physikalische Chemie*, **1963**, 67, 791-795.

[45] Bürgin, T.H.; Glaser, F.; Wenger, O.S.; Shedding Light on the Oxidizing Properties of Spin-Flip Excited States in a Cr^{III} Polypyridine Complex and Their Use in Photoredox Catalysis. *J. Am. Chem. Soc.*, **2022**, 144, 14181-14194.

[46] Connelly, N.G.; Geiger, W.E.; Chemical Redox Agents for Organometallic Chemistry. *Chem. Rev.,* **1996**, 96, 877-910.

[47] a) McDaniel, A. M.; Tseng, H.-W.; Damrauer, N.H.; Shores, M.P.; Synthesis and Solution Phase Characterization of Strongly Photooxidizing Heteroleptic Cr(III) Tris-Dipyridyl Complexes. *Inorg. Chem*., **2010**, 49, 7981-7991; b) Scarborough, C.C.; Lancaster, K. M.; DeBeer, S.; Weyhermüller, T.; Sproules, S.; Wieghardt, K.; Experimental fingerprints for

redox-active terpyridine in [Cr(tpy)2](PF6)n (n = 3-0), and the remarkable electronic structure of $[Cr(tpy)_2]^{1-}$. *Inorg. Chem.*, **2012**, 51, 3718-3732.

[48] Förster, C.; Heinze, K.; Photophysics and photochemistry with Earth-abundant metals – fundamentals and concepts. *Chem. Soc. Rev*., **2020**, 49, 1057-1070.

[49] a) Forlani, L.; Boga, C.; Del Vecchio, E.M.; Padovani, C.; Spontaneous oxidation of bis(heteroaryl)methanes and bis(heteroaryl)carbinols to ketones. ARKIVOC, **2004**, 15, 75-91. b) Avendaño, C.; Ramos, M.T.; Elguero, J.; Jimeno, M.L.; Bellanato, J.; Florencio, F.; Tautomerism of bis(2-benzothiazoly1)methanes. *Can. J. Chem.*, **1988**, 66, 1467-1473. c) Sterckx, H.; De Houwer, J.; Mensch, C.; Herrebout, W.; Abbaspour Tehrani, K.; Maes, B. U. W.; Base metal-catalyzed benzylic oxidation of (aryl)(heteroaryl)methanes with molecular oxygen. Beilstein *J. Org. Chem*. **2016**, 12, 144-153.

[50] a) Takamuku, T.; Tabata, M.; Yamaguchi, A.; Nishimoto, J.; Kumamoto, M.; Wakita, H.; Yamaguchi, T.; Liquid Structure of Acetonitrile−Water Mixtures by X-ray Diffraction and Infrared Spectroscopy. *J. Phys. Chem*, **1998**, 102, 8880-8888. b) Ewing, M.B.; Ochoa, J.C.S.; Vapor Pressures of Acetonitrile Determined by Comparative Ebulliometry. *J. Chem. Eng. Data*, **2004**, 49, 486-491.

[51] a) Farran, R.; Le-Quang, L.; Mouesca, J-M.; Maurel, V.; Jouvenot, D.; Loiseau, F.; Deronziera, A.; Chauvin, J.; $[Cr(ttpy)_2]^{3+}$ as a multi-electron reservoir for photoinduced charge accumulation. *Dalton Trans*., **2019**, 48, 6800-6811. b) Wang, M.; Weyhermüller, T.; England, J.; Wieghardt, K.; Molecular and electronic structures of six-coordinate "low-valent" $[M((Me)bpy)_3]^0$ (M = Ti, V, Cr, Mo) and $[M(tpy)_2]^0$ (M = Ti, V, Cr), and seven-coordinate $[MoF((Me)bpy)_3](PF_6)$ and $[MX(tpy)_2](PF_6)$ (M = Mo, X = Cl and M = W, X = F). *Inorg. Chem*., **2013**, 52, 12763-12776.

[52] Deposition numbers 2260441 for $[Cr^{III}(bik)_3](OTf)_3$ (**1**), 2260442 for $[Cr^{III}(bim)_3](OTf)_3$ (**2**), 2260443 for $[Cr^{III}(bie)_3](BF_4)_3$ (**3**) and 2260444 (for $[\{Cr(bim)_2\text{-}\mu OH\}_2]^{4+}$) contain the supplementary crystallographic data for this paper. These data are provided free of charge by the joint Cambridge Crystallographic Data Centre and Fachinformationszentrum Karlsruhe Access Structures service.

SYNOPSIS TOC:

For table of content only

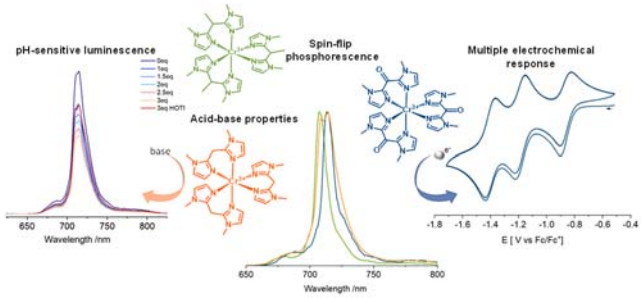

In a context of search for abundant phosphorescent emitters, this study details the photophysics properties of the first series of homoleptic tri(didentate) Cr(III) complexes with 6-membered chelate ring, in addition to their electrochemical and acid-base properties. Althogether, it offers new insights for the design of photoactive Cr(III) complexes relying until now mainly on tri(didentate) complexes with 5-membered chelate ring and di(tridentate) complexes with 6-membered chelate ring.